

## The formation and differentiation of magmas

### Bezmen N.I, Gorbachev P.N. Experimental study of gabbro-syenite melt differentiation in superliquidus conditions on the example of Northern Timan massife.

Institute of Experimental Mineralogy RAS, Chernogolovka Moscow district (bezmen@iem.ac.ru)

**Abstract.** In this work we experimentally studied the interaction of gabbro-syenite melt corresponding to the average composition of Northern Timan rocks with a complex hydrogen-containing magmatic fluid at 1000° C and 400 MPa. The composition of the magmatic fluid closed to natural has controlled by the special cell in high gas pressure vessel. In superliquidus conditions the initial melt exfoliate in the melts of different composition, forming a contrast, cryptic and rhythmic melt stratification of the samples. The temperature gradients are absent in the natural hypabyssal conditions, as a result of gravitational migration of nano-clusters of different densities are formed the convection cells. Thereby, as a result of our experimental data in absence of temperature gradients an initial fluid melt is completely differentiated in liquid state. As the migration of fluid components in the upper part of the massife the processes of crystallization are activated from the bottom to the top of the magma chamber.

**Keywords:** *experiment, gabbro-syenite, differentiation melts, superliquidus, contrast, cryptic, rhythmic melt stratification.*

#### Introduction

Alkaline rocks are multicomponent systems and in many cases are exceptionally rich in volatile components, especially H<sub>2</sub>, H<sub>2</sub>O, CO<sub>2</sub>, F, P and S, which play an important role in their genesis. The complexity of studying alkaline rocks in the presence of magmatic fluid was the reason for conducting experimental studies on the phase relationships between minerals and melts, mainly in "dry" conditions. The purpose of our research was to study the differentiation of the alkaline melt in superliquidus conditions under the pressure of a complex, near-natural, magmatic fluid, applied to a particular gabbro-syenite massif of Northern Timan.

#### Experimental method

As a rule, the fluid phase of alkaline massifs contains water, hydrogen, fluorine and other fluid components, so the experiments were carried out in a high-gas pressure vessel with controlled fugacity of gases in the H-O-C-F system, which are the main components of the magmatic fluid of the Northern Timan gabbro-syenite massif. The peculiarity of the experimental procedure was consisted in direct dosing of hydrogen in the fluid phase by the hydrogen diffusion through the walls of platinum capsules using the improved method of the membrane Shaw (Bezmen et al., 2016). The fugacity

of other gases in the H-O-C system was controlled by buffer reactions involving carbon. The scheme of a hydrogen cell with a charged capsule is described in detail in the works (Bezmen, 2001; Bezmen et al., 2016). The starting silicate sample was a column of glass prepared from oxides, corresponding to the bulk composition (Table 1) of the Northern Timan massif. To avoid the diffusion of iron into the platinum capsule from the melt during the run, the experiments were carried out in crucibles of vitreous graphite, which was simultaneously an indicator of the activity of carbon. The crucible was inserted into a platinum capsule with a diameter of 8 mm, a height of 50 mm with a wall thickness of 0.2 mm. Then water was poured into the capsule, the weight of which was determined by temperature and pressure and was 200 mg. The presence of water in the reaction capsule after the experiment was considered an indispensable condition for the reliability of the experiment. The welded capsule was inserted into a Re-reactor, which was filled by an argon-hydrogen mixture under a pressure of 100 atm with a given mole fraction of hydrogen. The composition of the fluid phase in the experiments was controlled by the fugacity of hydrogen and the presence of atomic carbon in the form of a crucible of glass graphite. The calculation of gases in the fluid phase was carried out on the assumption of an ideal mixture of real gases:  $X_{H_2O} = 0.29$ ;  $X_{H_2} = 0.12$ ;  $X_{CO_2} = 0.01$ ;

$$X_{CO} = 0.01; \quad X_{CH_4} = 0.57; \quad \log f_{O_2} = -14.2.$$

Calculations show that the experiment was carried out under oxidation-reduction conditions corresponding to the magnetite stability field (Bezmen et al., 2016). Besides 3.5 wt.% F as a fluoroplastic (C<sub>n</sub>F<sub>n+2</sub>) was added to the melt so far as the gabbro-syenite massif of Northern Timan contains the significant amounts of F-bearing hornblende and actinolite as well as accessory minerals such as fluorapatite and fluorite. The samples were analyzed by a wide probe (20-40 μm) on a scanning electron microscope (SEM) of Tescan Vega II XMU with energy-dispersive (INCAx-sight) and wave (INCA wave 700) X-ray spectrometers. The analyzes locations are shown by white circles and squares in the figures 1 and 2.

#### Experimental results

After the run, the sample was divided into three main zones (Table 1, Fig. 1, 2): alkaline-syenite in the lower part of the sample (II), an intermediate zone of gabbro-syenite composition (III) and predominantly alkaline gabbro in the upper zone (IV-V).

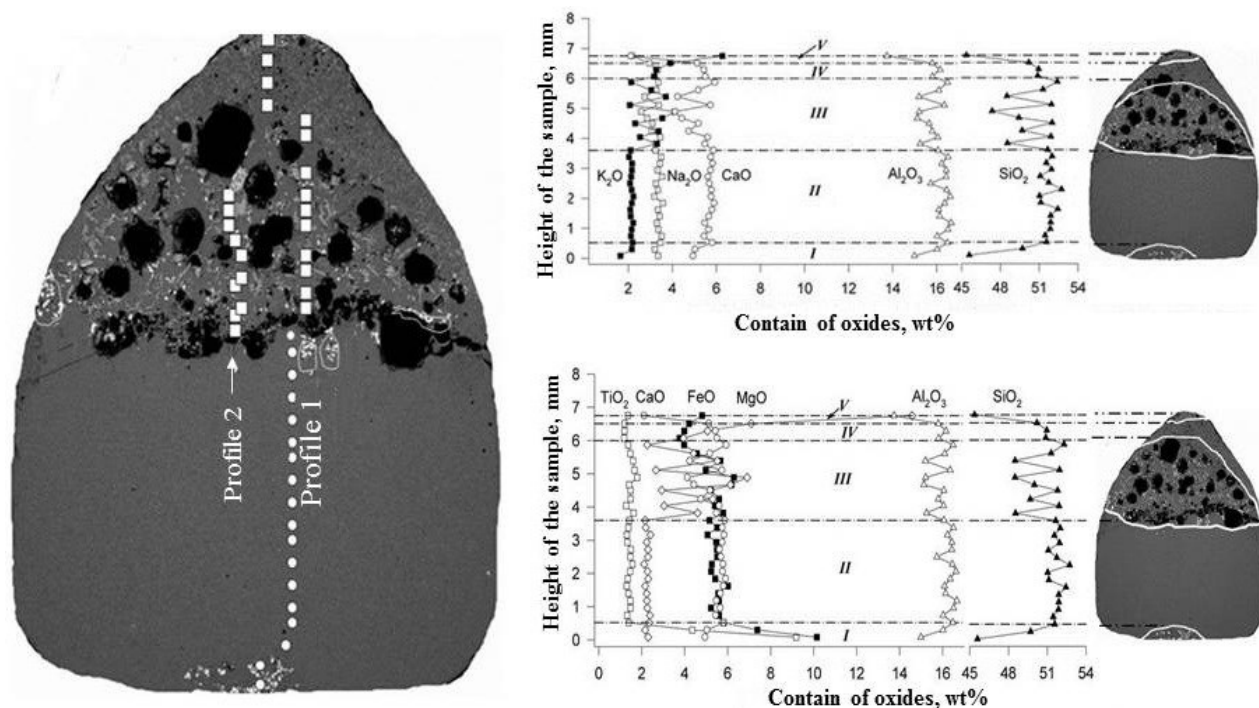


**Fig. 1.** *I* - alkaline gabbro-pyroxenite lens enriched with ilmenite and titanomagnetite globules; *II* - syenite layer; *III* - zone of rhythmically stratified gabbro-syenite with lenses of ore-bearing alkaline syenite melt. The black cavities of the fluid released during quenching; *IV* – cryptic differentiated alkaline gabbro layer; *V* - layer of alkaline amphibolite gabbro.

A melt of alkaline gabbro-pyroxenite (*I*) enriched in ore components (Tab. 1) became isolated in the syenite zone in the form of a lens. On the basis of the analysis of the parallel profiles 1 and 2 (Fig. 2) in zone (*III*) the rhythmically stratified layers of alkaline gabbro (*IIIa*) and alkaline syenite (*IIIb*, Tab. 1) were determined (Fig. 2). The isolated lenses of alkaline syenite (Fig. 1, 2) enriched by quenching titanomagnetite and ilmenite globules are chaotically

located in this zone. The average composition of these segregations is shown in Table 1 (*VI*). An alkaline gabbro zone (*IV-V* in Figs. 1 and 2) contains the needles of the quenching actinolite and brown hornblende the number of which are on the increase toward to the upper part of the sample in the form of a cryptic stratification up to the formation of alkaline gabbro-amphibolite (*V*, Tab. 1).

**Table 1. Compositions of glasses obtained as a result of differentiation of the initial gabbro-syenite melt.**

Components	Started composition	<i>I</i>	<i>II</i>	<i>III</i>	<i>IIIa</i>	<i>IIIb</i>	<i>IV</i>	<i>V</i>	<i>VI</i>
SiO <sub>2</sub>	52.23	45.60	51,73	49.93	47.36	50.74	50.68	45.37	49.40
TiO <sub>2</sub>	2.06	9.19	1,41	1.52	1,79	1,37	1.20	1.36	5.03
Al <sub>2</sub> O <sub>3</sub>	15,69	14.99	16.31	15.72	15.21	16,49	15.92	13.74	15.56
FeO	9.51	10.15	5,46	5.37	6.29	3.97	3.98	4.81	7.32
MnO	0.15	0.24	0.12	0.08	0.08	0.05	0.13	0.04	0.09
MgO	4.55	2.30	2.26	4.26	6.91	2,25	5.36	14.58	2.27
CaO	4.59	4.94	5.72	5.06	4.12	5,93	5.35	2.11	5.08
Na <sub>2</sub> O	3.02	3.35	3.38	3.10	2,58	3,36	3.17	2.17	3.49
K <sub>2</sub> O	2.36	1.64	2.14	2.93	4.10	2,13	3.45	6.27	1.95
F	0	4.14	3.30	4.22	4.89	3,62	3.92	6.04	3.19
H <sub>2</sub> , H <sub>2</sub> O, CO <sub>2</sub> , CO <sub>2</sub> , CH <sub>4</sub> *	0	3.46	7,78	7.96	7.08	10.09	6.38	3.51	6.39
Total sum	97.59	100	100	100	100	100	100	100	100

\*) Approximate content of fluid components by completing up to 100% microprobe analysis.

*I, II, III, IV, V* - average compositions of standed apart melts as a result of the experiment, see text.

*IIIa, IIIb* - composition of the upper rhythm, a-layer of syenite, b - layer of alkaline gabbro.

*VI* - average compositions of syenite lenses enriched with ore components (ilmenite and titanomagnetite globules).

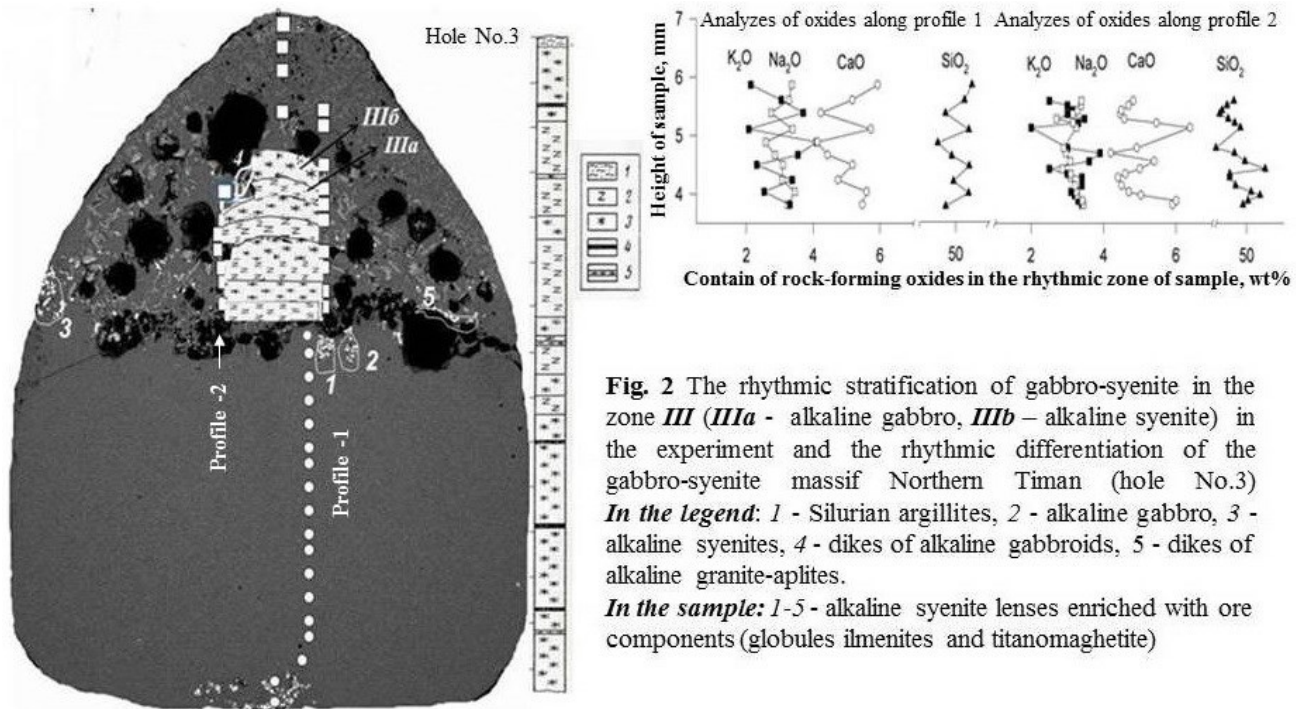


**Fig. 2** The rhythmic stratification of gabbro-syenite in the zone III (IIIa - alkaline gabbro, IIIb – alkaline syenite) in the experiment and the rhythmic differentiation of the gabbro-syenite massif Northern Timan (hole No.3)  
**In the legend:** 1 - Silurian argillites, 2 - alkaline gabbro, 3 - alkaline syenites, 4 - dikes of alkaline gabbroids, 5 - dikes of alkaline granite-aplites.  
**In the sample:** 1-5 - alkaline syenite lenses enriched with ore components (globules ilmenites and titanomaghetite)

**Mechanism of superliquidus nano-cluster differentiation of fluid melts**

The key to understanding the mechanism of magmatic differentiation is knowledge of the silicate melt structure. The magmatic melts are always saturated by the fluid components which strongly influence on the properties of the melts: liquidus temperature, viscosity, thermal conductivity, polymerization, entropy and other thermodynamic properties. In this connection in the fluid-containing magmatic melts at temperatures above the liquidus, polymolecular nano-sized clusters are formed (Bezmen, 2001). According to modern data on the *in situ* study of fluid metal systems, clusters represent an intermediate state of matter between a liquid and crystals and have a layered structure (jellium" model; Cohen, Knight, 1990), an ordered core and a shells composed of OH, H<sub>2</sub>, Cl, F, CO, CO<sub>2</sub>, Cr<sub>2</sub>O<sub>3</sub>, P<sub>2</sub>O<sub>5</sub> etc. which stabilize the existence of clusters over time. In previous studies the nano-cluster differentiation of the fluid-bearing melts it was shown by electron microscopy that clusters have a pseudocrystalline core surrounded by fluid components with generally dimensions of 6-10 nm (Bezmen, 2001). In accordance with the thermodynamics of irreversible processes (Glensdorf, Prigogine, 1973) the certain groups of fluctuating nano-clusters are capable of gravitationally moving in a depolymerized melts with the formation of a cryptic, rhythmic and contrasting stratification. It is especially important to emphasize that the separation effect is observed at constant temperature.

Thus, as seen in Fig. 1 and 2, the layers and lenses of the contrast composition melts as well as the cryptic stratification of the alkaline gabbro (IV-V) melt are formed as a result of the flotationally gravitational migration of fluid-silicate nano-clusters during the run. The elevated titanium contents are confined to the melts of alkaline gabbro-pyroxenite (I) in the syenite zone (II) and to the rhythmically stratified gabbro-syenite zone (III) in the form of separate alkaline syenite lenses (Fig. 2).

Usually, the rhythmic stratification in magmatic melts is associated with thermal and mass transfer arising as a result of thermal or chemical gradient (density), which formed the D-D type of convective cells (Frenkel, 1995). The silicate rocks are characterized by low thermal conductivity. Therefore, at the hypabyssal conditions of the massifs formation the temperature gradients are hundredths and tenths of a degree. Such temperature gradients are incapable to lead to the appearance of convection cells in the magma chamber of thermal type. The study of the analytical data along the profile 1 of the fluid-saturated gabbro-syenite zone (III) showed that the glasses are rhythmically stratified with the formation of alternating melts of alkaline gabbros and syenites (Fig. 1). We conducted an additional analytical study of the glasses in the zone (III) along the profile 2 parallel to profile 1 in order to finally verify the correctness of this conclusion. It can be seen that the microanalysis data along the profiles 1 and 2 as a whole coincide with minor deviations (Fig. 2). Thus, the main factor of

convection is the difference in the density of nano-clusters. As a result, the stratified layers of different density and magmatic melts of the different composition are appeared accordingly. The experimental results and natural data coincided completely (Fig. 2).

Considering the various mechanisms of magmatic stratification in the experiment, we came to the conclusion that at hypabyssal conditions of the massif formation a density convective differentiation of the fluid magmatic melt arises as a result of gravitational migration of nano-clusters of different densities. Thus, in non-gradient conditions the high-fluid magmatic melts completely differentiated in liquid form. As the fluid components migrate both by themselves and in the fluid shells of migrating clusters, the effects of stratification are further developed under the influence of fluid inflow in the upper part of the magmatic chamber. In the lower parts of the magmatic chamber the crystallization processes are activated from the bottom upward due to the formation of solidus areas during the dissipation of fluid components from the melt.

### References:

1. Bezmen, N.I. (2001) Superliquidus differentiation of fluid-bearing magmatic melts under reducing conditions as a possible mechanism of formation of layered massifs: experimental investigations // *Petrology* 9 (4), 345–361.
2. Bezmen N. I., Gorbachev P. N., Martynenko V. M. (2016) Experimental Study of the Influence of Water on the Buffer Equilibrium of Magnetite–Wüstite and Wüstite–Metallic Iron // *Petrology* 24 (1), 84–99.
3. Cohen M.L., Knight W.D. (1990) The physics of metal clusters // *Physics Today* 12 42-50.
4. Glansdorff, P., Prigogine, I. (1971) Thermodynamic Theory of structure, Stability, and Fluctuation, N. Y.: Wiley 251 p.
5. Frenkel M.Ya. (1995) Thermal and chemical differentiation of the basic magmas. M.: Nauka, 239 p.

### **Kotelnikov A.R.<sup>1</sup>, Suk N.I.<sup>1</sup>, Kotelnikova Z.A.<sup>2</sup>, Yanev Y.<sup>3</sup>, Encheva S.<sup>3</sup>, Ananiev V.V.<sup>4</sup> Investigation of liquid immiscibility in fluid-magmatic systems.**

<sup>1</sup>Institute of Experimental Mineralogy RAS, Chernogolovka Moscow district,

<sup>2</sup>Institute of Geology of Ore Deposits, Petrography, Mineralogy, and Geochemistry, RAS, Moscow,

<sup>3</sup>National museum “Earth and People”, Sofia,

<sup>4</sup>Institute of Volcanology and Seismology FEB RAS, Petropavlovsk-Kamchatsky, Bulgaria (kotelnik@iem.ac.ru, sukni@iem.ac.ru, kotelnik@igem.ru)

**Abstract.** Melting in the system trachyrhyolite – water – salt (NaF, Na<sub>2</sub>CO<sub>3</sub>) has been investigated. Experiments were produced in high gas pressure vessel at special regime. It was obtained the immiscible splitting into two melts: L<sub>2</sub> which forms drops in matrix (L<sub>1</sub>). Drops composition is similar to composition of matrix and differs only in content of water, TiO<sub>2</sub> and alkaline and alkaline-earth elements relations. Phase distribution of ore elements (Rb, Cs, Sr, Cr, Fe, Nb, Mo, La, W) has been studied. Based on the analytical data the partition coefficients of the main elements between phases L<sub>1</sub> and L<sub>2</sub>  $K=[C_i(L_2)/C_i(L_1)]$  have been calculated. It has been obtained the following partition coefficients of oxides: K<sub>2</sub>O – 1.3; Rb<sub>2</sub>O – 2.0; Cs<sub>2</sub>O – 2.1; SrO – 0.99; FeO – 3.0; Cr<sub>2</sub>O<sub>3</sub> – 7.4; Nb<sub>2</sub>O<sub>5</sub> – 10; WO<sub>3</sub> – 21; MoO<sub>3</sub> – 26; La<sub>2</sub>O<sub>3</sub> – 30.

**Keywords:** experiment, melt, liquid immiscibility, trachyrhyolite, partition coefficients

Liquid immiscibility phenomenon is quite often observed in volcanic rocks and appears in presence of drops with distinct phase boundaries. Usually compositions of matrix and inclusions are practically identical. To model this phenomenon the experiments with trachyrhyolite samples of Bulgaria kindly submitted by prof. Y. Yanev have been produced. Melting in the system trachyrhyolite – water has been experimentally investigated. The powder of trachyrhyolite (composition, wt.%: Na<sub>2</sub>O – 2.97(19); MgO – 0.15(6); Al<sub>2</sub>O<sub>3</sub> – 11.51(12); SiO<sub>2</sub> – 72.78(13); K<sub>2</sub>O – 5.53(11); CaO – 1.05(7); TiO<sub>2</sub> – 0.13(6); FeO – 0.80(29)) was used as starting material. Weighed portions of trachyrhyolite powder (100 mg) were loaded into Pt-capsules with addition of calculate amount of water. Some amounts of oxides or salts of following elements: Rb, Cs, Sr, Cr, Fe, Nb, Mo, La, W – were added as indicative components. Total sum of additions don't exceed 2.5 wt % of trachyrhyolite charge. The balance sample / fluid was ~7.

Experiments were produced in high gas pressure vessel at special regime: (1) T=1200°C; P=5 kbar; time of exposure: 6 hours → (2) cooling up to T=1000°C; P=1 kbar; time of exposure: 48 hours → isobaric quenching.

At T=1200°C and P=5 kbar the melting, homogenization and fluid saturation of aluminosilicate melts were produced and as a result the porous glass was obtained. After parameters decreasing up to 1000°C and 1 kbar the melt heterogenization with arising of liquid immiscibility took place. It has been shown that in the system trachyrhyolite – water liquid immiscibility is exist as drops (phase L<sub>2</sub>) generation in basic melt volume (phase L<sub>1</sub>) (fig. 1).

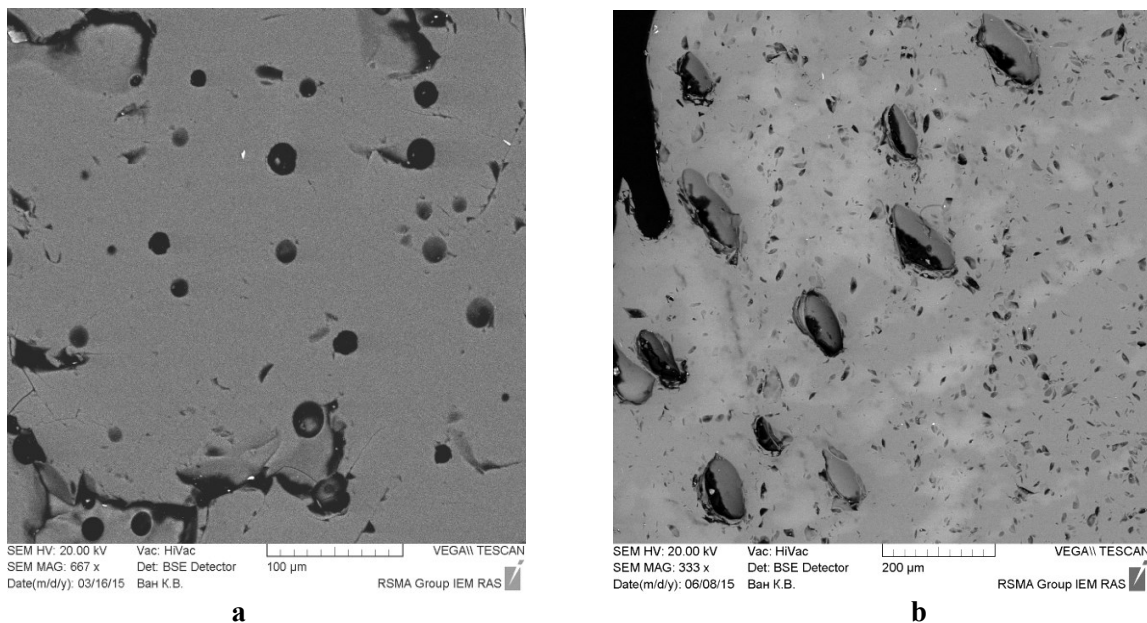


Fig. 1. Homogeneous glass obtained during trachyrhyolite melting at 1200°C and 5 kbar (a) and liquid immiscibility obtained during trachyrhyolite melting in conditions imitated volcanic process (decreasing of T P-parameters up to 1000°C and 1 kbar) (b).

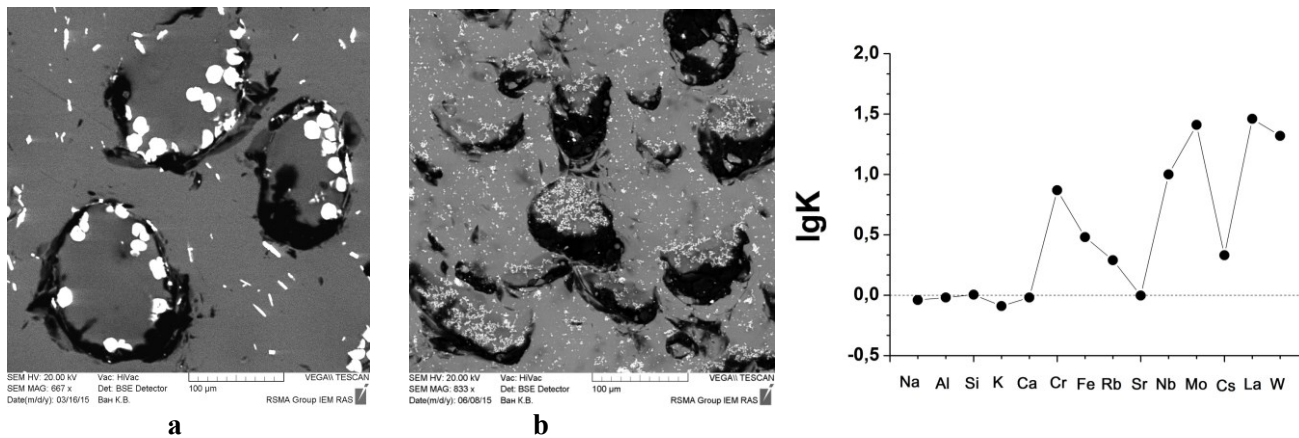


Fig 2. Liquid immiscibility in experiments of trachyrhyolite melting with La, Nb, Sr additions (a) and with Cr and Fe additions (b).

Fig. 3. Partition coefficients (lgK) of ore and petrogenic elements between phases L<sub>1</sub> and L<sub>2</sub>.

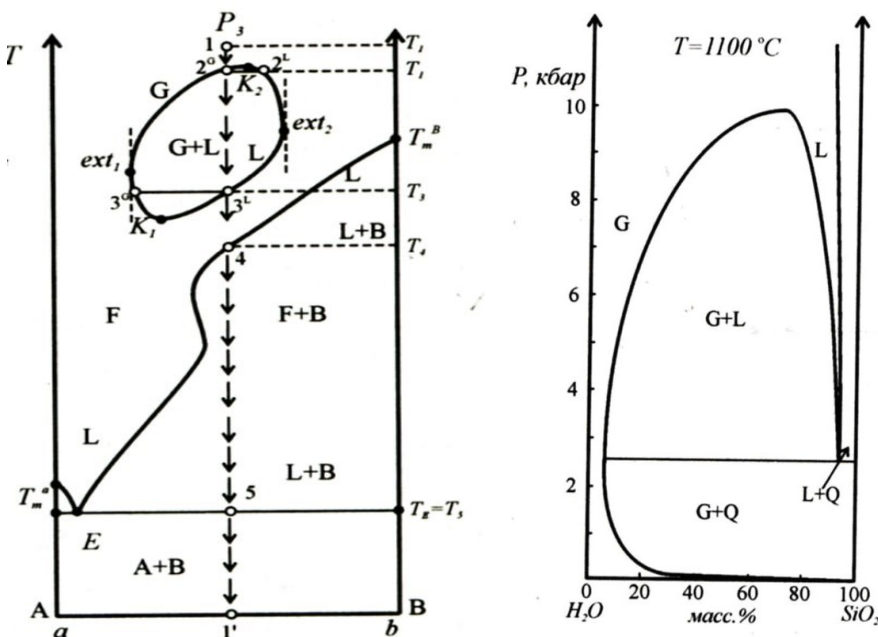


Fig. 4. Phase TX- and PX-diagrams of “silicate – fugitive” systems according (Zharikov, 2005).

Oxide	6936	6929	6937	6938	6939
	K <sup>1)</sup>	K <sup>2)</sup>	K <sup>1)</sup>	K <sup>1)</sup>	K <sup>1)</sup>
Na <sub>2</sub> O	1.37	1.20	0.64	0.71	0.62
MgO	-	0.71	-	-	3.2
Al <sub>2</sub> O <sub>3</sub>	1.07	1.07	0.92	0.83	0.85
SiO <sub>2</sub>	1.04	1.06	1.03	0.85	1.02
K <sub>2</sub> O	0.82	0.91	1.26	0.98	1.44
CaO	0.92	0.97	0.94	1.04	0.94
TiO <sub>2</sub>	1.00	-	≈3	0.60	0.64
Cr <sub>2</sub> O <sub>3</sub>	-	-	-	7.43 <sup>2)</sup>	-
FeO	1.05	1.02	2.01	4.25 <sup>2)</sup>	3.32
Rb <sub>2</sub> O	-	-	1.97	-	-
SrO	1.14	0.84	-	-	-
Nb <sub>2</sub> O <sub>5</sub>	-	≈10 <sup>2)</sup>	-	-	-
MoO <sub>3</sub>	-	-	-	-	1.11 <sup>3)</sup>
Cs <sub>2</sub> O	-	-	2.15	-	-
La <sub>2</sub> O <sub>3</sub>	-	≈29 <sup>2)</sup>	-	-	-
WO <sub>3</sub>	-	-	-	-	1.64 <sup>3)</sup>

The drops composition is similar to melt's composition and distinguishes from melt by other contents of water, TiO<sub>2</sub> and another proportions of alkaline- and alkaline-earth elements. At the diagram (fig. 2) the glasses obtained in experiments with addition of oxides Nb, La (a) and Cr, Fe (b) are presented. Composition of basic melt (matrix) (fig. 2a) is (wt %): SiO<sub>2</sub> – 67.56; Al<sub>2</sub>O<sub>3</sub> – 10.65; Na<sub>2</sub>O – 2.80; K<sub>2</sub>O – 5.23; CaO – 0.89; SrO – 1.29; Nb<sub>2</sub>O<sub>5</sub> – 0.73; La<sub>2</sub>O<sub>3</sub> – 0.40. Drops composition is (wt %): SiO<sub>2</sub> – 71.72; Al<sub>2</sub>O<sub>3</sub> – 11.40; Na<sub>2</sub>O – 3.36; K<sub>2</sub>O – 4.76; CaO – 0.86; SrO – 0.99; Nb<sub>2</sub>O<sub>5</sub> – 1.00; La<sub>2</sub>O<sub>3</sub> – 0.52.

Indicative components (Rb, Cs, Sr, Cr, Fe, Nb, Mo, La, W) began redistribute between phases L<sub>1</sub> and L<sub>2</sub> when liquid immiscibility was arise.

Based on the analytical data the partition coefficients of the main elements between phases L<sub>1</sub> and L<sub>2</sub>  $K=[C_i(L_2)/C_i(L_1)]$  have been calculated. Following partition coefficients of oxides have been obtained: K<sub>2</sub>O – 1.3; Rb<sub>2</sub>O – 2.0; Cs<sub>2</sub>O – 2.1; SrO – 0.99; FeO – 4.2; Cr<sub>2</sub>O<sub>3</sub> – 7.4; Nb<sub>2</sub>O<sub>5</sub> – 10; WO<sub>3</sub> – 21; MoO<sub>3</sub> – 26; La<sub>2</sub>O<sub>3</sub> – 29 (tabl. 1, fig. 3).

Efficiency of extraction process of ore elements (La, Mo, W, Nb, Cr) in conditions of liquid immiscibility existence in fluid-magmatic systems has been shown.

Layering obtained in our experiments is according to phase diagram “silicate – fugitive” (Zharikov, 2005) or layering of L<sub>1</sub>+L<sub>2</sub> type indicative for the system PQ-type (fig. 4). Trachyrhyolite melt represents salt of II-type. Apparently such phenomena can distinct appear only in volcanics as a result of there fast eruption and quenching in subsurface conditions. Based on the experimental and theoretical data we have developed schematic PX-diagram of pseudobinary granite – water system (fig. 5).

**Table 1. Partition coefficients of components**

$$K=[C_i(L_2)/C_i(L_1)]$$

<sup>1)</sup>  $K=(C_i^{L_2})/C_i^{L_1}$ , concentrations C<sub>i</sub> for elements oxides; L<sub>1</sub> – “water phase” of silicate melt; L<sub>2</sub> – drops of silicate melt with low water content;

<sup>2)</sup> partition coefficients of Nb and La oxides, Cr and Fe oxides calculated taking into account the quantity of lanthanum-niobates crystals and chromites in phases L<sub>1</sub> and L<sub>2</sub>;

<sup>3)</sup> partition coefficients calculated taking into account the quantity of Mo-sheelite crystals in phase L<sub>2</sub>; partition coefficients for Mo and W are following:

$$K=(C_{MoO_3}^{L_2})/C_{MoO_3}^{L_1} \approx 26.3;$$

$$K=(C_{WO_3}^{L_2})/C_{WO_3}^{L_1} \approx 20.9.$$

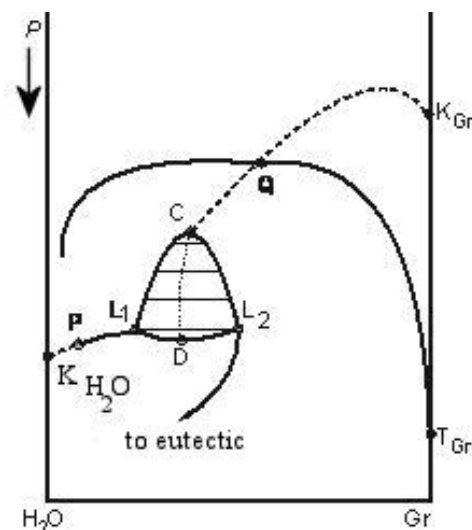


**Fig. 5. Scheme of phase equilibria in high temperature part of pseudobinary system water – model granite (P-X section) developed taking into account particularities of P-Q systems with liquid layering.** Heavy lines – compositions of liquid phases correspond to three phase's equilibria, dotted line – critical curves. Thin line – isobaric sections. P and Q – lower and upper critical points in presence of solid phase; K<sub>H<sub>2</sub>O</sub> and K<sub>Gr</sub> – critical points of water and granite; T<sub>Gr</sub> – triple point of granite; L1 and L2 – equilibria of two liquids, gas and solid phase Gr ending in point C; equilibria of two liquids and gas ending in point D.

**Conclusions**

1. In conditions imitated volcanic process (T=1200 → 1000°C; P= 5 → 1 kbar) in the trachyrhyolite – water system the liquid immiscibility has been obtained.

2. It has been shown that compositions of coexisting aluminosilicate phases are quite identical (except for alkaline elements). This fact allows to explain liquid immiscibility phenomenon in terms of

phase diagram of PQ-type in the area of PT-parameters lower Q point.

3. Distribution of number elements (La, Nb, Sr, W, Mo, Cr, Fe, Rb, Cs) between phases L<sub>1</sub> and L<sub>2</sub> has been experimentally investigated. It has been shown that ore elements predominantly concentrate in phase L<sub>2</sub>.

4. The data obtained allow to estimate a probability of processes of ore material concentration and accumulation in distinct phases in fluid-magmatic systems during their intrusion (upraise).

This study was supported by RFBR, project № 15-05-03393.

*Authors are grateful to N.I. Kuznetsov and A. Terekhin for engineering and technical services and carrying out the experiments in high gas pressure vessel of IEM RAS.*

Reference:

1. V.A. Zharikov. Foundation of physical geochemistry. M: Moscow University: Nauka, 2005. 654p.

**Shubin I.I.<sup>1</sup>, Zharkova E.V.<sup>2</sup>, Koptev-Dvornikov E.V.<sup>1</sup> Minerals of Kivakk mafic-ultramafic filled intrusion (Northern Karelia). Experimental determination of intrinsic oxygen fugacity**

<sup>1</sup> M.V. Lomonosov Moscow State University, Department of Geology, Moscow, <sup>2</sup> V.I. Vernadsky Institute of Geochemistry and Analytical Chemistry RAS, Moscow ([shubin.ivann@mail.ru](mailto:shubin.ivann@mail.ru)).

**Abstract.** The work is devoted to studying the stratified intrusion of the Kivakka type and determination of intrinsic oxygen fugacity ( $fO_2$ ) of minerals. The Kivakka intrusion is located in North Karelia on the north-western shore of the lake Piaozero. It is part of the Olang group of stratified peridotite-gabbro-noritic intrusions, which is part of the sub latitudinal band of basite-hyperbasite massifs. Pure grains of olivines (Ol), and orthopyroxenes (Opx) were selected for the experiment. The intrinsic oxygen fugacity measured for orthopyroxenes lies in the buffer equilibrium region of wustite-magnetite (WM) and below, while  $fO_2$  for olivine at 800°C lies below the buffer equilibrium quartz-fayalite-iron (QFI), and at 1100°C crosses the quartz-fayalite-magnetite (QFM).

*Keywords: intrinsic oxygen fugacity, olivine, orthopyroxene, Kivakka.*

Intrinsic oxygen fugacity so as temperature and pressure, is one of the fundamental conditions of formation and evolution of magmatic rocks. This is due to the increased attention to the problem many researchers Earth Sciences. Rate of oxygen fugacity in two ways, namely by using thermodynamic

analysis of mineral equilibrium rocks deep origin and directly own volatility definition pilot oxygen minerals deep origin using solid phase electrolytic cells (Sato M.).

This work is dedicated to the experimental measurement of oxygen fugacity in minerals Kivakk mafic-ultramafic intrusive, using solid electrochemical cells. The samples were chosen for the research Kivakk mafic-ultramafic laminated intrusive of the intrusive, due to the fact that this mass of carefully studied and there is a huge stone and analytical material on this object. The results of the experiment will expand the database on that array and possibly help you refine the model and conditions of formation of this array.

Kivakk mafic-ultramafit laminated intrusive is included in Olangsk group of laminated peridotite-gabbro-norit intrusives belonging to sub latitudinal rail bazit-giperbazit mass. (Bychkova Y.V., Koptev-Dvornikov E.V. 2004). Geographically, this intrusive is located on the Northwestern shore of Lake Pyaozero in North Karelia. Containing rocks are represented adergneissed biotite and amfibole gneiss, gneissose granite and granodioorto gneiss the upper Archean.

Definition of own volatility oxygen olivins and orthopyroxenes have been carried out on high-temperature installation based on two solid electrolytes at temperature from 800<sup>0</sup>C up to 1050<sup>0</sup>C at a pressure of 1atm. Temperature measurement accuracy was  $\pm 2^0C$ , own oxygen fugacity  $\pm 0.2 \log fO_2$ . (Kadik, A.A., Zharkova, E.V.et al.1988).

In the texture Kivakk of the intrusive on mineral composition can be divided into several zones: the lower at-contacting, olivinit, norit, norit-gabbro, gabbro-norit with pigeonite, the top at-contacting. Bottom up section there is a shift to a laminated Series through interbedding with paragenesis cumulative change reversed (from the gabbro-norit to olivinit). For measurements of samples were taken from the olivinit zone (KV 410 Ol), from a small zone interbedding bronzite and harzburgite in the upper part of the olivinit zone (KV 419 Opx), norit zone (KV 420 Ol,Opx and K V 438 Opx). The measurement results are listed below (table 1).

**Table1. The values of the coefficients "A" and "B" in empirical dependencies  $\log fO_2 = A-B/T$  (K).**

Sample	A	B	r	n	$\log fO_2$ at 1040°C
410 Ol	32,921	57979	0,986	7	-11,72
419 OPx	12,510	33286	0,980	7	-12,69
420 Ol	23,881	46858	0,975	7	-11,71
420 OPx	22,300	45025	0,989	7	-11,84
438 OPx	13,128	34195	0,992	7	-14,21

r-coefficient of correlation, n - number of experimental points.

## The formation and differentiation of magmas

As a result of the experiments it has been shown that intrinsic oxygen fugacity of pyroxenes lies in the area of the buffer equilibrium wüstite-magnetite (WM) and the intrinsic oxygen fugacity of olivines at temperatures below 800°C lies below the buffer equilibrium of quartz-iron-fayalite (QFI), and at temperatures above 1100°C crosses the curve balance quartz-fayalite-magnetite (QFM).

The temperature equilibrium for olivine and orthopyroxene (sample KV 420) is 940.1°C ± 2°C.

The values obtained intrinsic oxygen fugacity (Tab.1) compared with the values of the oxygen fugacity obtained using the KOMAGMAT program (Koptev-Dvornikov, oral presentation). Normative content of Rock-forming minerals in the explored samples (Koptev-Dvornikov et al., 2001), measured values and volatility of log  $fO_2$  oxygen, obtained in a realistic model of the formation of Kivakk intrusive are listed in table 2.

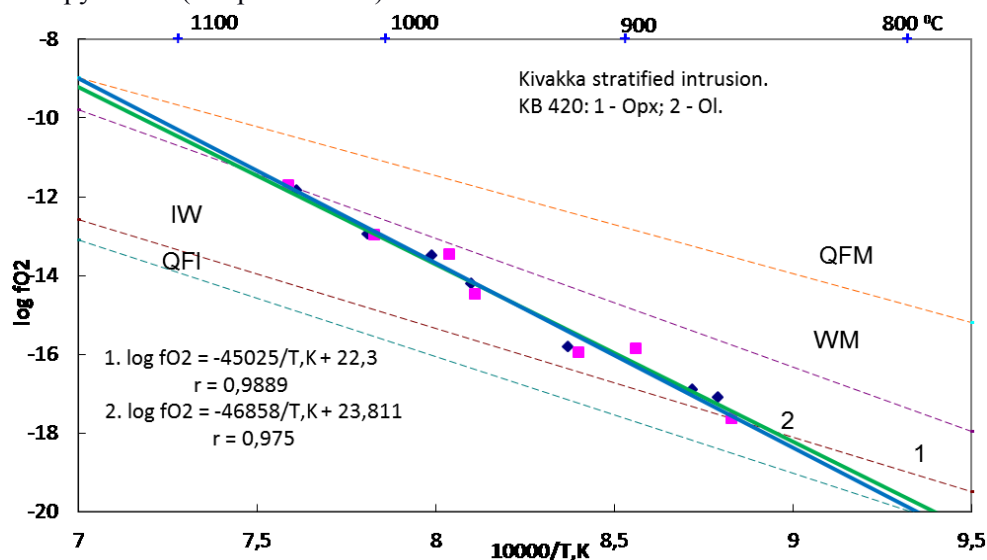
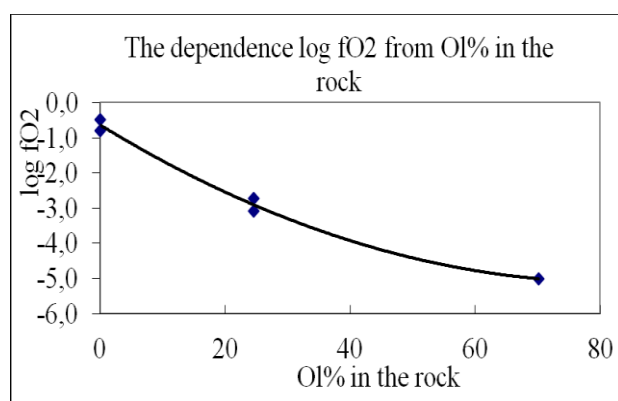


Figure 1. Experimentally determined log  $fO_2$  v.s.  $10^4/T^0 K$  (KV-420).

Table 2. Comparison of experimental data with the model.

	Pl	CPx	OPx	OI	log $fO_2$ ex p.	log $fO_2$ mod.
410 Ol	11,5	3,4	14,8	70,2	-5,4	-10,38
419 OPx	58,9	14,9	25,3	0	-9,7	-10,50
420 Ol	20	4,4	50,9	24,6	-7,4	-10,48
420 OPx	20	4,4	50,9	24,6	-7,8	-10,48
438 OPx	58,7	7,2	32,4	0	-9,9	-10,36

fugacity minerals. Clearly this relationship is shown in Figure 1. 2. significant Correlation with a probability of at least 99% figure 2 correlation between its intrinsic oxygen fugacity and volatile content of olivine in the breed.



The data obtained suggest that rocks piled minerals, crystallize, oxygen fugacity in the chamber close to the volatility, calculated in a realistic model of the formation of Kivakks intrusive obtained using KOMAGMAT. At the same time in rocks that contain olivine intratelluric oxygen markedly higher fugacity, and there is an empirical relationship between the content of olivine and its own oxygen

### References:

1. Bychkova Y.V., Koptev-Dvornikov E.V. 2004 Rhythmic layering of the Kivakka type: Geology, petrography, petrochemistry, and a hypothesis for its formation. *Petrology*. V. 12, No 3. P. 244-264.
2. Kadik, A.A., Zharkova, E.V. et al. 1988. Redox Conditions in the Upper Mantle: Experimental Determination of Oxygen Fugacity in the Minerals of Peridotite Xenoliths from Shavaryn-Tsaram Volcano, Mongolia, *Geokhimiya*, No. 6, P. 783-799.
3. Koptev-Dvornikov E.V., Kireev B.S. et al. 2001 Distribution of cumulative mineral assemblages, major and trace elements over the vertical section of the Kivakka intrusion, Olanga group of intrusions, northern Karelia. *Petrology*. V. 9, No1. P. 3-27.
4. Sato M. Intrinsic oxygen fugacities of iron-bearing oxide and silicate minerals under low total pressure. *Geol. Soc. Am. Mem.* 1972. Vol.135. P.289-307.

**Solovova I.<sup>1</sup>, Yudovskaya M.<sup>1</sup>, Borisovskiy S.<sup>1</sup>, Zinovieva N.<sup>2</sup> Thermometric study of microinclusions in olivine of Uitkomst massive, Transvaal.**

<sup>1</sup> Institute of Geology of Ore Deposits, Petrography, Mineralogy, and Geochemistry, RAS, Moscow, ([solovova@igem.ru](mailto:solovova@igem.ru)),

<sup>2</sup> M.V. Lomonosov Moscow State University, Department of Geology, Moscow

**Abstract.** The inclusions in the cumulative olivine of ultramafites of the Uitkomst sill in the Bushveld complex were studied. It is established that the parent melt correspond to high-magnesian andesibasalt with low water content and increased alkalinity. Its crystallization temperature is close to 1450°C. Coexisting inclusions of the second type have an acid composition and a homogenization temperature in the range of 1170-1210°C. It is shown that initially they were crystalline inclusions of albite. The composition of the melt varies depending on the degree of the secondary alteration of albite, the crystallization and size of the inclusion. It is assumed that an increased concentration of alkalis in the melt of primary inclusions and a change in the composition of the crystalline inclusions of albite is connected with the influence of hot Na-K-H<sub>2</sub>O fluid with dissolved petrogenic components during or after crystallization of the liquidus olivine at the bottom of the magma chamber.

**Keywords:** layered ultramafic complexes, inclusions, fluid, thermometry, parent melt

The study of layered intrusions of the world showed that they have a complex structure and a Precambrian age. The richest deposits of elements of the platinum group, Cr, V and Cu-Ni sulfides are associated with layered complexes. The Bushveld complex among others is one of the oldest (2050 million years), with a maximum output area and ore occurrences. However, the question of the genesis and composition of the primary magmas of Bushveld is still debatable (Wilson, 2012; Yudovskaya et al., 2013). The compositions of fresh fine-grained marginal sills within the intrusions are extremely diverse and can not be considered as analogues of the original magmas. To solve this problem, researchers used modeling programs (Harmer, Sharpe, 1985, Barnes et al., 2010; Davies, 1982). The method of experimental study of microinclusions in minerals is additional to solving this problem. The study of the rocks of the subvolcanic Uitkomst sill, genetically related to Bushveld, is of particular interest. It is assumed that such sills are the only medium where melt inclusions could be preserved in primitive rocks.

We studied the inclusions in the cumulative olivine of ultramafic rocks, in the central part of the sill section (Fo 90-92, NiO до 0.50 мас.%, CaO до 0.15 мас.%). Crystallized inclusions of 30-50 μm in

size, according to classical criteria, correspond to primary melt (Fig. 1, series I, view at 20°C). The combined inclusions of spinel + melt coexist with these inclusions (Fig. 1, series II, view at 20°C). Melt inclusions contain idiomorphic daughter phases, among which olivine and orthopyroxene were determined. During the high-temperature experiments, melting of daughter phases with the appearance of a melt and separation of the fluid phase as a gas bubble was observed. At a maximum experimental temperature of 1430°C, complete homogenization of the inclusions was not achieved. A similar process was observed in the silicate part of the combined inclusions, which additionally confirms the primacy of the melt inclusions coexisting with them.

Melt compositions of high-temperature inclusions (> 1430°C) are characterized by a high content of MgO, up to 18 wt% (Table 1). They are practically dry - the concentration of H<sub>2</sub>O is 0 - 0.2 wt%. Melts contain SiO<sub>2</sub> 54-57 wt% and can be considered as high-magnesian andesite or andesibasalt and close to the model compositions of the primary magmas of Bushveld. The main difference is the extremely high concentration of alkalis (up to 5 wt%) with Na>K. There is a low content of CaO, not more than 3.6 wt%.

Inclusions of the second type in the size of 5-50 microns there are also in the cumulative olivine. They differ in all characteristics from the first type. Inclusions often have a crystallographic facet (Fig. 2a). Small inclusions are pure, without signs of crystallization, the composition responds to albite. These inclusions remained unchanged at heating. Larger inclusions are finely crystallized in varying degrees. Due to the small size of the phase, they were identified qualitatively and correspond to albite, Cl-apatite, sphene (in Si, Ca, Ti), perovskite (in Ti, Ca), amphibole, rutile, ilmenite. The inclusions were homogenized at a temperature in the range of 1170-1210°C.

The compositions of the obtained melts (Table 2) are characterized by a high concentration of SiO<sub>2</sub> - up to 65 wt %, alkalis (Na<sub>2</sub>O + K<sub>2</sub>O up to 8 wt %) and Al<sub>2</sub>O<sub>3</sub> (up to 15.7 wt %). They contain not less than 1 wt % water. The high content of fluid in the melt is confirmed not only by the presence of Cl- and H<sub>2</sub>O-containing daughter phases in the inclusions, but also by the behavior of the inclusions during the experiments - melting of the phases leads to the appearance of abundance of fluid bubbles (Fig. 2e).

## The formation and differentiation of magmas

**Figure 1.** View of primary melt (series I) and combined (series II) inclusions in olivine under a microscope, transparent light. At a temperature of 1310°C, the primary inclusion contains a melt, fluid phase and up to 20 vol % of the incompletely melted daughter crystals of olivine and orthopyroxene. The beginning of melting of the silicate part of the combined inclusion (series II) is clearly fixed at 1130°C. A rise in temperature to 1330°C leads to decrepitation and the formation of halo of matter loss around the vacuole. L – melt, Fl – fluid, Sp – spinel, Sil – silicate part of the combined inclusion, Ol – olivine, Opx – orthopyroxene.

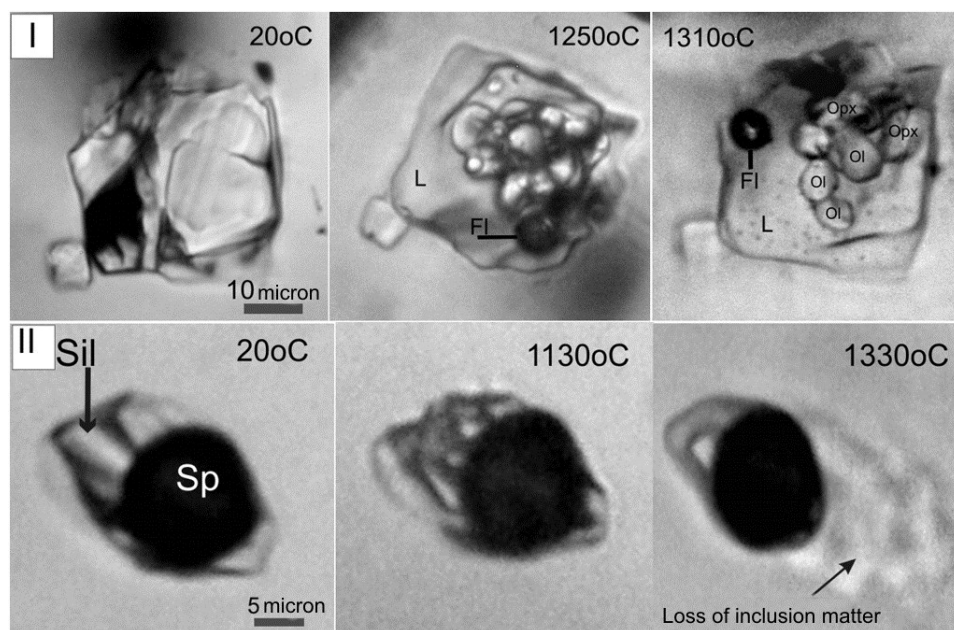


**Table 1. Compositions of high-temperature melt inclusions in olivine of Uitcomst ultramafites and model compositions of primary magmas of Bushveld, wt%**

	1	2	3	4	5	6
SiO <sub>2</sub>	54.23	55.58	56.90	55.15	54.95	55.24
TiO <sub>2</sub>	0.07	0.25	0.13	0.31	0.34	0.38
Al <sub>2</sub> O <sub>3</sub>	9.75	12.24	9.48	10.61	11.25	12.13
FeO	9.64	5.66	7.74	9.50	9.61	9.2
MgO	18.05	16.60	17.61	14.63	13.29	12.97
MnO	0.10	0.10	0.14	0.18	0.18	0.15
CaO	3.65	2.52	3.59	6.16	6.39	6.84
Na <sub>2</sub> O	3.40	3.58	3.17	1.60	1.51	1.75
K <sub>2</sub> O	1.11	1.46	0.81	0.79	0.85	0.88
Na <sub>2</sub> O+	4.51	5.03	3.97	2.39	2.36	2.63
K <sub>2</sub> O						
T, °C	1360	1325	1365	H&S	B	D

**Note.** 1-3 - melt inclusions; 4-6 - model compositions of primary magmas Bushveld. H&S – (Harmer, Sharpe, 1985), B – (Barnes et al., 2010), D – (Davies, 1982).

A different pattern was observed for the K/Na ratio. Melts of all inclusions, both acid and high-magnesian, lie on a single trend. It is assumed that this situation is possible if Na-K-rich hot fluids containing dissolved petrogenic components are influenced to them during or after the crystallization of early olivine at the bottom of the magmatic chamber. An additional confirmation of this is the presence of abundance sub-parallel chains of minute ( $\leq 1$  micron) fluid inclusions in olivine (Fig. 2c).

**Table 2. Compositions of low-temperature inclusions in olivine, wt %**

	1	2	3
SiO <sub>2</sub>	65.03	64.50	64.80
TiO <sub>2</sub>	0.15	0.08	0.16
Al <sub>2</sub> O <sub>3</sub>	15.66	15.04	15.09
FeO	2.96	4.11	4.18
MgO	5.89	7.17	7.36
CaO	2.32	1.89	1.92
Na <sub>2</sub> O	6.56	6.53	5.16
K <sub>2</sub> O	1.21	1.29	1.27
Na <sub>2</sub> O +	7.77	7.82	6.43
K <sub>2</sub> O			

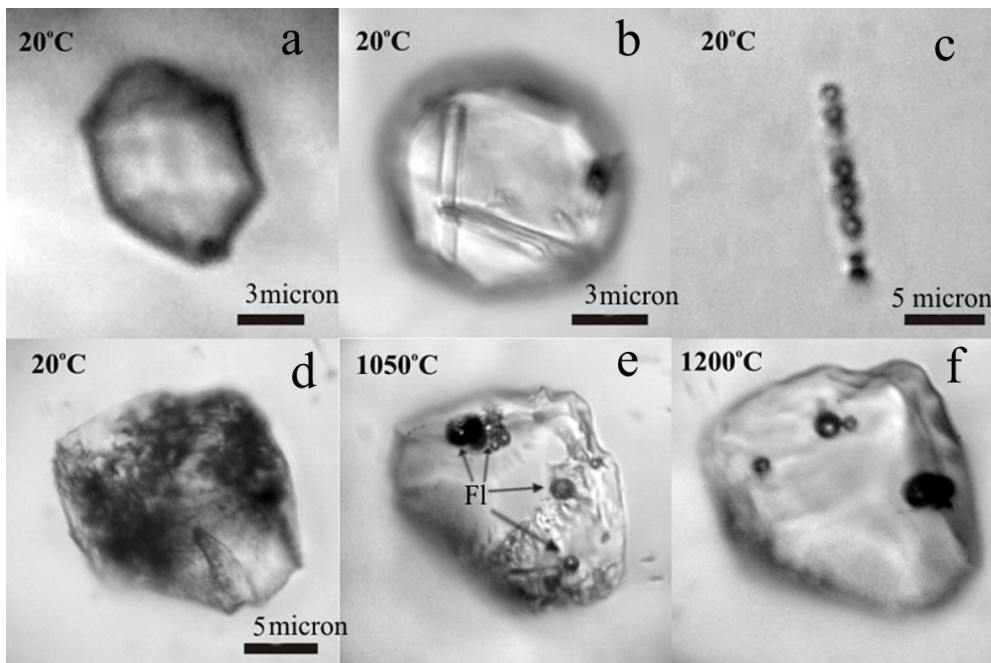


**Figure 2.** View of inclusions under a microscope, transparent light. a - inclusion with crystallographic faceting without crystallization, b - inclusion containing single crystalline phases (Cl-Ap and ore phase), c - a chain of fluid inclusions in olivine (x1500, oil immersion), d-f - phase changes in natural-crystallized inclusion at heating up to 1200°C. At 1050°C inclusion contains a melt, incompletely melted daughter crystalline phases and 8 fluid bubbles.

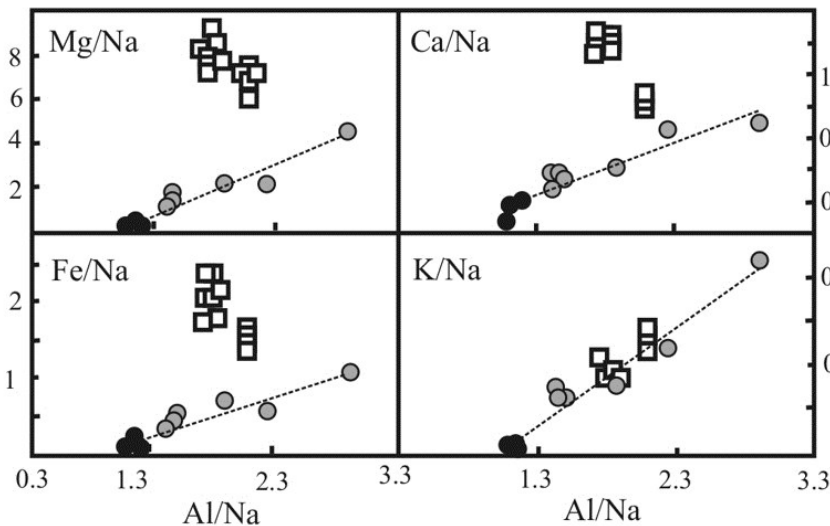


**Figure 3.** Variation of Na - normalized paired ratios of elements (mole ratios) in coordinates Me/Na - Al/Na. Highly magnesian melts - squares, acid compositions - gray circles. Albite - black circles.

References:

Since all inclusions contain anomalously high concentrations of alkalis, we considered variations of the pair ratios of elements normalized to Na (Fig. 3). It was found that if high-magnesian inclusions form compact fields, then inclusions of acid melts, including albite, fall on a single trend. Their position on the diagram depends on the degree of initial crystallization and the size of the inclusions, as well as on the homogenization temperature.

**Acknowledgment.** *The authors acknowledge partial support of M.V. Lomonosov Moscow State University (Program of Development). Quantitative chemical analyses were carried out in wavelength-dispersion mode, using a Superprobe JEOL JXA-8230 (Laboratory of High Spatial Resolution Analytical Techniques, Department of Petrology, Geological Faculty, Moscow State University) operated under the following conditions*

1. Barnes C.-J., Maier W., Curl, E. Composition of the marginal rocks and sills of the Rustenburg Layered Suite, Bushveld Complex, South Africa: Implications for the formation of the platinum-group element deposits. *Econ. Geol.* 2010. 105. 1491-1511.
2. Davies G., Cawthorn R. G., Barton J., Morton M. Parental magma to the Bushveld Complex. *Nature.* 1980. 287, 33-35.
3. Harmer R., Sharpe M. Field relations and strontium isotope systematics of the marginal rocks of the eastern Bushveld Complex. *Econ. Geol.* 1985. 80. 813-837.
4. Wilson A. A (2012) Chill Sequence to the Bushveld Complex: Insight into the First Stage of Emplacement and Implications for the Parental Magmas. *J. Petr.* 53 (6). 1123-1168
5. Yudovskaya M. A., Kinnaird J. A., Sobolev A. V., Kuzmin D. V., McDonald L. Wilson A. H. Petrogenesis of the Lower Zone Olivine-Rich Cumulates Beneath the Platreef and Their Correlation with Recognized Occurrences in the Bushveld Complex. *Econ. Geol.* 2013. 108 (8). 1923-1952.

**Suk N.I.<sup>1</sup>, Kotelnikov A.R.<sup>1</sup>, Peretyazhko I.S.<sup>2</sup>, Savina E.A.<sup>2</sup> Experimental study of melting of trachyrhyolite from Central Mongolia.**

<sup>1</sup> Institute of Experimental Mineralogy RAS, Chernogolovka Moscow district,

<sup>2</sup> A.P. Vinogradov Institute of Geochemistry SB RAS, Irkutsk (sukni@iem.ac.ru, kotelnik@iem.ac.ru, elen\_savina@mail.ru)

**Abstract.** Experimental study of melting of trachyrhyolite was produced in high gas pressure vessel in presence of 10 wt% H<sub>2</sub>O at two regimes: 1) at T=1250°C and P=5.5 kbar during of 6 h; 2) melting at T=1250°C and P=5.5 kbar (duration of 2 h) and then parameters were reduced to T=900°C and P=1 kbar (duration of 4 days). Starting materials were: trachyrhyolites of three types differ by F content (0.58, 2.45, 15.0 wt %) and mixtures of trachyrhyolites with minimum and maximum F contents in ratio 1:1, 2:1 and 1:2. It was obtained the immiscible splitting into aluminosilicate and fluoride-calcium melts which was observed when F content in the system was >5 wt%. Study of REE (La, Ce, Y, Gd, Dy) distribution between immiscible phases shows that REE predominantly concentrate in fluoride melt.

*Keywords:* experiment, melt, liquid immiscibility, trachyrhyolite, partition coefficients, effusive rocks

It has been investigated melting of trachyrhyolites discovered among effusive rocks of Nilginsky depression in Central Mongolia and belong to dzunbainsky suite of early Cretaceous. In trachyrhyolites of one of overtrusters the rocks anomaly enriched in Ca and F were discovered. In these rocks content of CaO and F run to 15-20 and 10-15 wt % respectively. To study trachyrhyolites of three types were selected. They differ in F content (0.58, 2.45 and 15.0 wt %). In thin sections these rocks have not symptoms of secondary changes and presented by light-gray or light-lilac porphyric rocks with phenocrysts of quartz and feldspars (sanidine). Mineral composition of selected rocks is identical and differs only in fluorite content.

**Experimental method**

Trachyrhyolite melting was produced in high gas pressure vessel in presence of 10 wt% H<sub>2</sub>O at two regimes: 1) at T=1250°C and P=5.5 kbar during of 6 h; 2) melting at T=1250°C and P=5.5 kbar (duration of 2 h) and then parameters were reduced to T=900°C and P=1 kbar (duration of 4 days) and then isobaric quenching was produced. The triturations of trachyrhyolites of three types with different F content (0.58, 2.45 and 15 wt%) or mixtures of trachyrhyolites with minimal and maximal F content in proportions 1:1, 2:1 and 1:2 were used as starting materials.

Experiments to study phase distribution of REE have been produced in high gas pressure vessel at T=1250°C and P=5.5 kbar during of 6 h with addition

of REE (La, Ce, Y, Gd, Dy) oxides (1 mg for each). The experimental samples were analyzed on a digital scanning electron Tescan Vega II XMU microscope.

**Table 1. Compositions of initial F-contained trachyrhyolites of Mongolia (wt%).**

N	Mn1354	Mn1120	Mn1247
SiO <sub>2</sub>	48.96	71.62	74.86
TiO <sub>2</sub>	0.15	0.19	0.21
Al <sub>2</sub> O <sub>3</sub>	7.96	10.99	11.74
Fe <sub>2</sub> O <sub>3</sub>	0.34	0.67	0.70
FeO	0.30	0.80	0.63
MnO	0.06	0.09	0.05
CaO	22.76	5.27	1.21
MgO	-	0.03	0.05
K <sub>2</sub> O	3.56	4.75	5.10
Na <sub>2</sub> O	2.59	3.46	3.60
Li <sub>2</sub> O	0.0082	0.0097	0.012
Rb <sub>2</sub> O	0.014	0.022	0.023
P <sub>2</sub> O <sub>5</sub>	0.05	0.03	0.03
F	15.0	2.45	0.58
H <sub>2</sub> O <sup>-</sup>	0.09	0.21	0.11
H <sub>2</sub> O <sup>+</sup>	0.90	1.36	1.47
CO <sub>2</sub>	0.17	<0.05	<0.05
∑(I)	102.51	101.89	100.38
O=2F	6.32	1.03	0.24
∑(II)	96.19	100.86	100.14

**Experimental data**

At T=1250°C and P=5.5 kbar in the sample with maximum F content (15 wt %) it has been obtained liquid immiscibility between silicate and fluoride-calcium melts, which produce drops of one liquid in another (fig. 1). Trachyrhyolites with F content of 0.58 and 2.45 wt % were melted forming homogeneous glass.

Second series to study trachyrhyolite melting was produced in conditions imitated volcanic process i.e. in decrease of temperature and pressure which is typical for the process of the magma rise to the earth surface and its eruption (T=1250°C, P=5.5 kbar => T=900°C, P=1 kbar).

In the sample of trachyrhyolite with maximum F content liquid immiscibility between silicate and fluoride-calcium melts appeared too, but segregations of immiscible phases were smaller (fig. 2) which approached experimental samples to natural trachyrhyolite image.

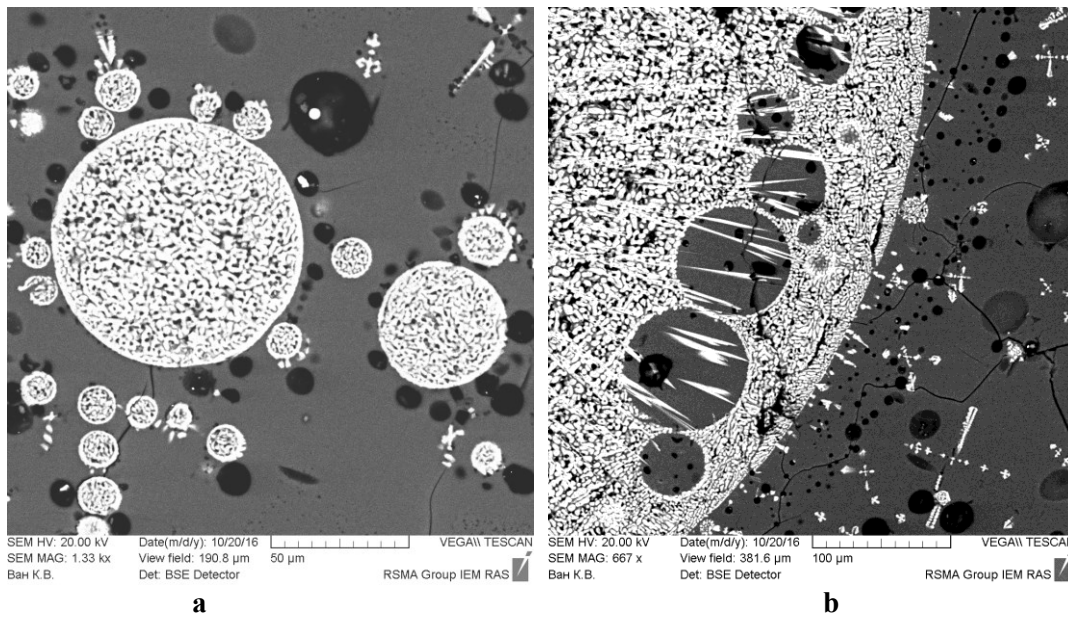


**Fig. 1.** Liquid immiscibility between silicate (dark) and fluoride-calcium (light) melts, obtained at T=1250°C and P=5.5 kbar. BSE image.

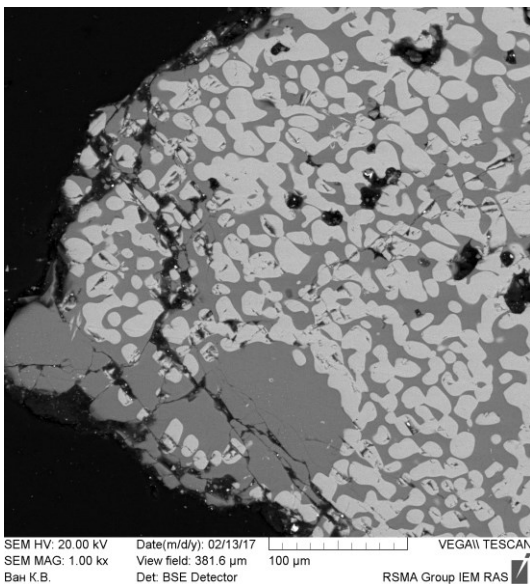


**Fig. 2.** Liquid immiscibility between silicate (dark) and fluoride-calcium (light) melts, obtained in conditions with decrease of temperature and pressure (T=1250°C, P=5.5 kbar => T=900°C, P=1 kbar). BSE image.

To estimate the minimum F concentration when liquid immiscibility can arise in the system the experiments with mixtures of trachyrhyolites with minimum and maximum F contents in ratio 1:1, 2:1 and 1:2 have been produced at T=1250°C and P=5.5 kbar. Calculated F contents in the samples studied were 7.27, 5.15 and 9.40 wt % approximately. In all experiments liquid immiscibility was obtained (fig. 3). But in the sample with 5.15 wt % F content minimum amount of drops of fluoride-calcium phase was observed. These data show that liquid immiscibility can arise when the system contain F content >5 wt %.

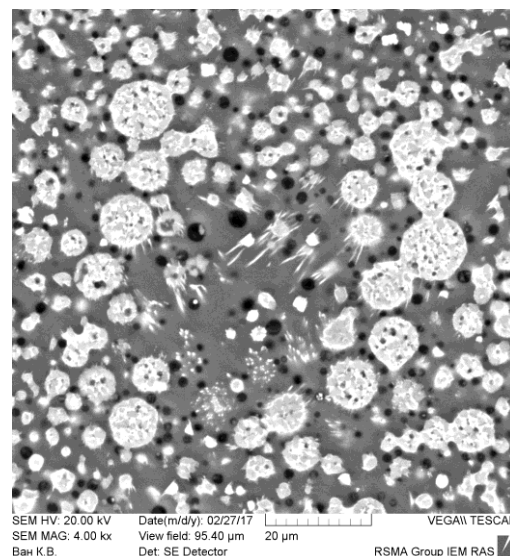


**Fig. 3.** Liquid immiscibility between silicate (dark) and fluoride-calcium (light) melts, obtained during melting of mixtures of trachyrhyolites with minimum and maximum F contents in ratio 1:2 (9.40 wt % F) at T=1250°C and P=5.5 kbar. BSE image.

Investigation of REE (La, Ce, Y, Gd, Dy) distribution between layered phases at  $T=1250^{\circ}\text{C}$  and  $P=5.5$  kbar showed that they predominantly concentrate in fluoride melt. Preliminary estimations of partition coefficients of REE between aluminosilicate melt and fluoride-calcium phase ( $K_i^{\text{REE}}=C_i^{\text{LF}}/C_i^{\text{Sil}}$ ) show that they are for Y ~ 20, La – 20-40, Ce – 15-30, Gd – 20-30, Dy – 16-20.

In the sample with minimum F content (5.15 wt %) the emulsion looked like drops with 1-1.5  $\mu\text{m}$  in size has been distinctively observed (fig. 4). This phase was enriched in REE. Amount of this phase strongly decreases with increase of F content in the system. Mechanism of arising of such emulsion is apparently analogical to mechanism of titanate-silicate liquid immiscibility obtained by us previously (Suk, 2007, 2012).

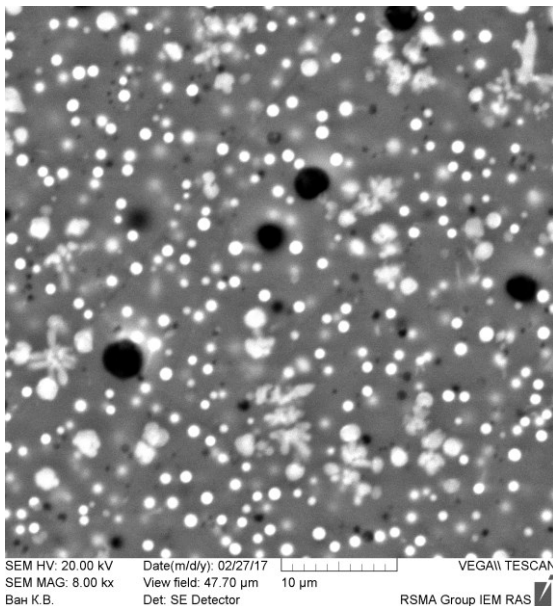


**Fig. 4.** Result of melting of mixtures of trachyrhyolites with minimum and maximum F contents in ratio 2:1 (5.15 wt % F) at  $T=1250^{\circ}\text{C}$  and  $P=5.5$  kbar. BSE image.

Petrographical observations and data of study of melting inclusions in minerals from trachyrhyolites evidence about coexistence of trachyrhyolite (aluminosilicate) and fluoride-calcium melts as at the stage of mineral phenocrysts growth in magma chamber so at lava eruption. This fact is proved out by our experimental investigations.

#### References:

1. Suk N.I. Experimental study of alkaline magmatic aluminosilicate systems with the connection of genesis of rare earth-niobium loparite deposits. Dokl. Akad. Sci. 2007. V. 414. N 2. P. 249-252.
2. Suk N.I. Liquid immiscibility in fluid-magmatic aluminosilicate systems containing Ti, Nb, Sr, REE and Zr (experiment). Petrology. 2012. V. 20. N 2. P. 156-165

## Azarova N.S., Bovkun A.V. Typomorphic features of oxide minerals from the groundmass of kimberlite rocks of Kimozero (Karelia)

*M.V. Lomonosov Moscow State University, Department of Geology, Moscow (nadiya-azarova@mail.ru)*

**Abstract.** The results of the survey are reported of quantitative relations, phase and chemical composition of oxide minerals of kimberlite genesis proper from the groundmass of kimberlite rock of Kimozero pipe (Karelia). A typical feature of the composition of microcrystals chromite from Kimozero kimberlites is the extremely low content of magnesium. This feature distinguishes it from chromspinel of the kimberlite genesis proper from the groundmass of Russian kimberlites and kimberlites from abroad, usually containing from 5 to 15 wt. % MgO.

**Keywords:** Kimozero pipe, kimberlite, groundmass, oxide minerals, ilmenite, spinel

Paleoproterozoic Kimozero kimberlites, located within the Karelian craton, are one of the oldest original diamondiferous rocks in the world. The age of their formation corresponds to  $1986 \pm 4$  million years (U-Pb dating of mantle zircons by the TIMS method) (Samsonov et al., 2009). Kimberlites contain diamond crystals larger than 1 mm (Ushkov et al, 1999), but the commercial significance of these rocks is still unclear.

The Kimozero occurrence is represented by a flattened elongated (~ 2 km) deposit and a series of steeply falling tubular bodies composed of kimberlite breccias, tuffs, massive kimberlites of at least two phases of intrusion (Ushkov, 2001, Putintseva, 2002, Putintseva et al., 2009, Ustinov et al. , 2009). Kimberlites penetrate the gabbro-dolerites of the Early Proterozoic and shungit-bearing terrigenous rocks of Iyedikovia (Onega Paleoproterozoic structure, 2011), they make up apophyses in them, contain a lot of their xenoliths and skalitites.

Petrographic features, chemical and phase compositions of oxide minerals have been studied in several samples of metamorphosed porphyritic massive kimberlites and kimberlite breccia of Kimozero, differing in the content of mica, carbonate, and ore minerals (Fig. 1). Porphyritic phenocrysts in the studied rocks are represented by pseudomorphs of serpentine in olivine up to 4 mm in size, as well as in large (up to 3 mm) grains of aluminomagnesiochromite, Mn-ilmenite and amphibole. In the groundmass of Kimozero kimberlites there's big amount of chlorite, serpentine and carbonates. Oxide minerals, apatite, baddeleyite, pentlandite, monazite and zircon are presented in a small amount. The kimberlite breccia differs from other studied samples with a low content of ore minerals and a wide occurrence of pseudomorphs of rutile and sphene in ilmenite and secondary iron oxides.

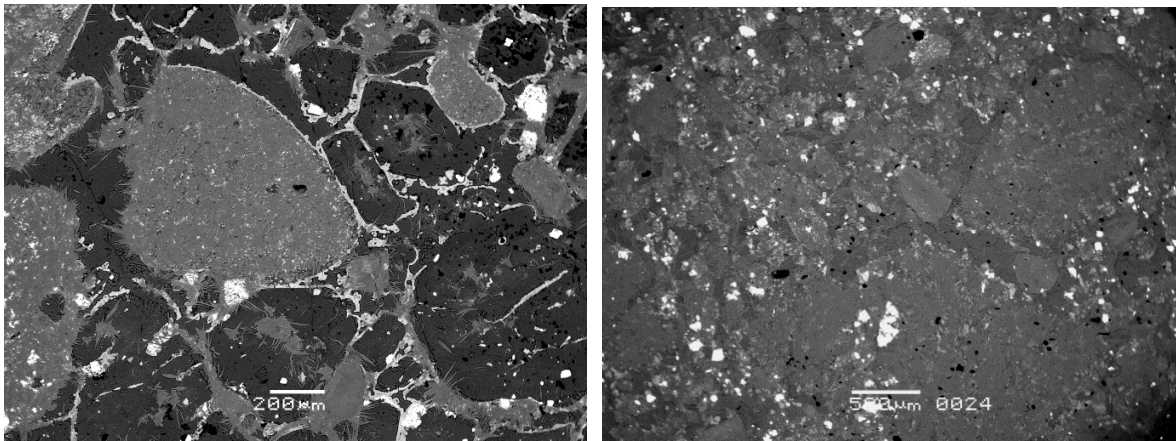


Fig. 1. Microphotograph of metamorphosed porphyritic massive Kimozero kimberlites. Images in reflected electrons

Oxide minerals in the studied rocks are represented by large (up to 3 mm) Mn-ilmenite grains (Fig. 2), alumomagnesio- and magnesiochromite, and small (<100 μm) secretions of Mn-ilmenite, chromspinelides, titanomagnetite and magnetite.

Mn-ilmenite is the most widespread among the oxide minerals, while spinelides prevail in the sample of kimberlite enriched with carbonate. In rocks containing amphiboles there is practically no ilmenite; oxide minerals are represented by chromspinel and products of ilmenite change

(rutile and sphene). Mn-ilmenite grains (up to 4.8 wt% MnO), in some cases, small grains are enriched with Nb<sub>2</sub>O<sub>5</sub> (up to 9 wt%), are often associated with monazite and usually contain thin decay structures represented by magnetite. The composition of large phenocrysts (up to 0.6 mm) of ilmenite with well-defined decay structures and small (up to 60 μm) grains in the groundmass of rocks are similar. In the sample of the kimberlite breccia (sample Kim-3), the secretions of ilmenite are almost completely replaced by rutile and sphene.

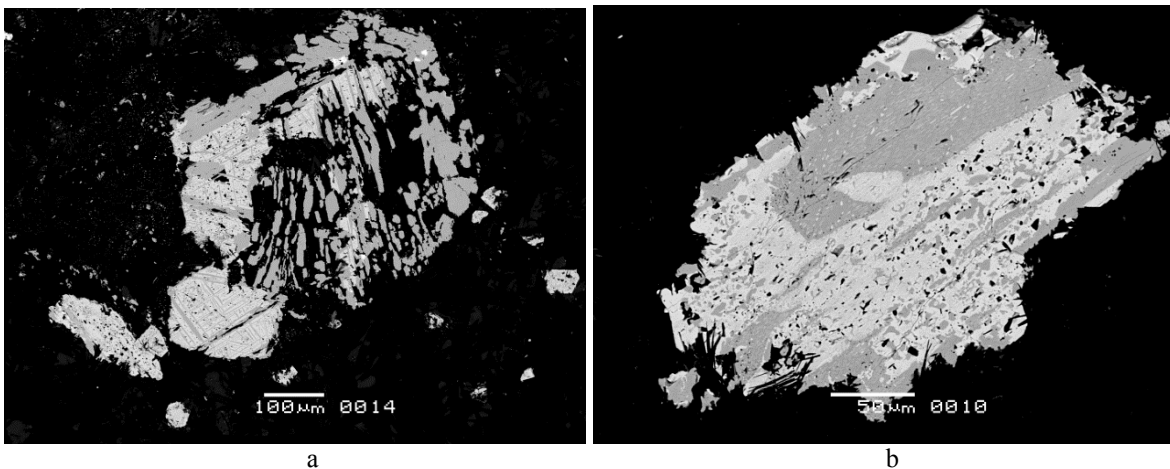


Fig.2. Grains of ilmenites with decay structures in Kimozero kimberlite. Images in reflected electrons

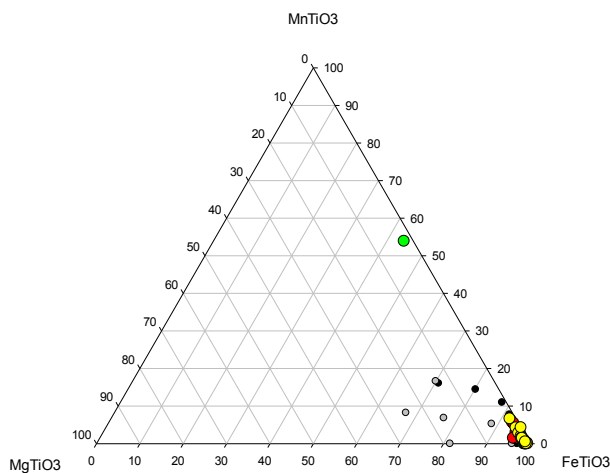


Fig.3. The diagrams of compositions in the coordinates of the main minerals (a) and impurity elements (b) for ilmenite from kimberlite rocks of Kimozero (large circles are the samples studied in this work, small gray and white circles are data of Putintseva and Spiridonov (2017))

Microcrystal chromspinelides are represented by idiomorphic zonal grains up to 60 μm in size, the centers of which are composed of Ti-containing chromite (up to 51.6 wt.% Cr<sub>2</sub>O<sub>3</sub>, 1.4-5.6 wt.% TiO<sub>2</sub>) with an MgO content of up to 0.8 wt.% , variable amounts of Al<sub>2</sub>O<sub>3</sub> (up to 11wt.%) and a constant admixture of MnO (up to 1.7wt.%) and ZnO (up to 3wt.% ). To the grain edge, the contents of Cr, Al and Ti decrease, and the amount of Fe<sup>3+</sup> increases. The grains of such chromite are usually surrounded

## The formation and differentiation of magmas

by wide (up to 40  $\mu\text{m}$ ) rims consisting of a fine-grained congeries of Mn-ilmenite, magnetite and / or Ti-magnetite with inclusions of baddeleyite and sulphide minerals.

In addition, the chromite described above forms rims around rounded phenocrysts of magnesiochromite and alumomagnesiochromite (up to 14.5 wt% MgO and 61 wt%  $\text{Cr}_2\text{O}_3$ ), probably having a xenogenic origin. The latter are sometimes

found in the form of small relics inside the grains of Ti-containing chromite poor in magnesium. The composition of phenocrysts and relics of magnesiochromite and alumomagnesiochromite is similar to the composition of spinels from diamondiferous lherzolites.

There are large grains of magnetite up to 0.5 mm in size.

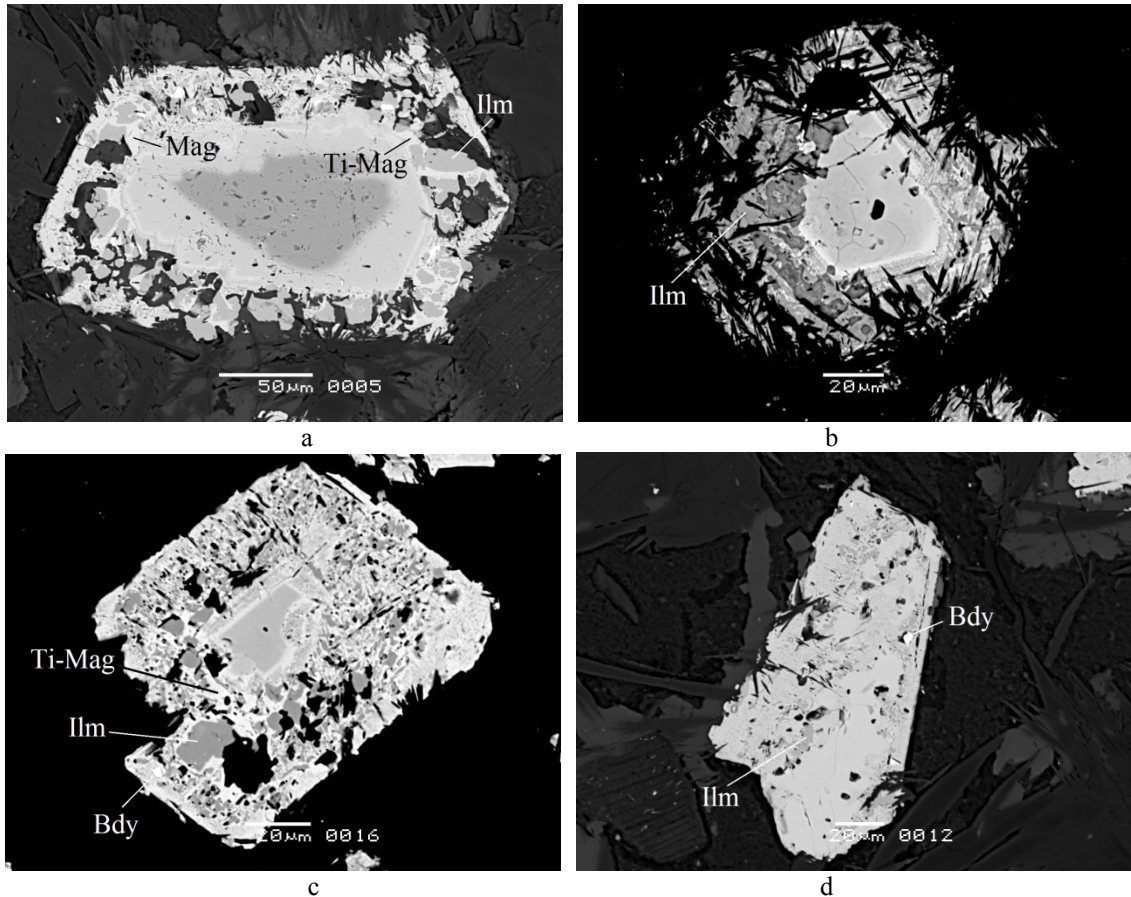


**Fig.4.** Chromspinelides with magnetite-ilmenite rims (a-c) and grains of magnetite with inclusion of baddeleyite and ilmenite (d) in the groundmass of Kimozero kimberlite. Images in reflected electrons

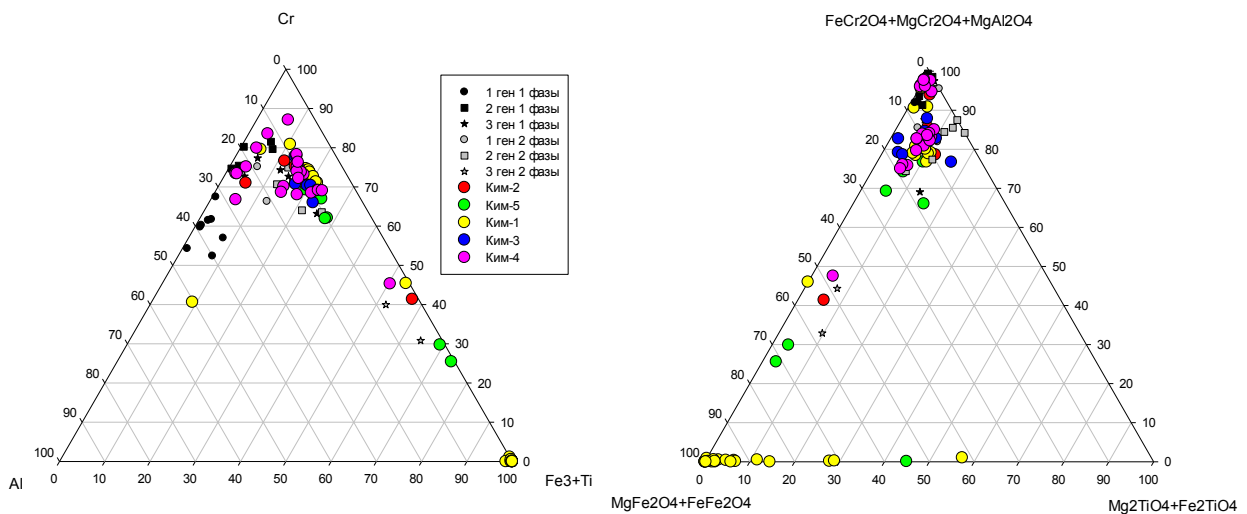


**Fig.5.** The diagrams of compositions in the coordinates of the main minerals (a) and impurity elements (b) for spinels from the groundmass of Kimozero kimberlite (large circles are the samples studied in this work, small gray and white circles are data of Putintseva and Spiridonov (2017))

**Conclusions**

A typical feature of the composition of microcrystals chromite from Kimozero kimberlites is the extremely low content of magnesium. This feature distinguishes it from chromespinels of the kimberlite genesis proper from the groundmass of Russian kimberlites and kimberlites from abroad, usually containing from 5 to 15 wt. % MgO. In addition, chromespinelides from Kimozero kimberlites are characterized by adulteration of MnO and ZnO. A high content of MnO (1.8-4.8 wt.%) is typical of the ilmenite of these rocks.

## References:

1. Onega Paleoproterozoic structure (geology, tectonics, deep structure and mineralogy) // Ed. L.V. Glushanin, A.I. Golubev, N.V. Sharov, V.V. Shchiptsov. Petrozavodsk: Karel. SC RAS. 431p.
2. Putintseva E.V. Geodynamic environment of formation of alkaline complexes of the Karelo-Kola region and features of their metallogeny: a new interpretation from the position of mantle plumes. In the book: Mantle plumes and metallogeny. Petrozavodsk-Moscow. 2002. P. 183-188.
3. Putintseva E.V., Spiridonov E.M. The oldest in Russia diamondiferous kimberlites and metakimberlites Kimozero, Karelia // *Izvestia VUZ. Geology and exploration*. 2017. In the press.
4. Putintseva E.V., Zhitnikova I.A., Polyakova E.I. and others. Assessment of the prospects of the diamondiferousness of Karelia // *Minerageny of the Precambrian*. Petrozavodsk. 2009. P. 203-205
5. Samsonov A.V., Larionova Yu.O., Salnikova E.B. Isotope geochemistry and geochronology of the Paleoproterozoic Kimberlites of the Kimozero occurrence (Karelia). Sec.: Mat. IV Ross. konf. isotope. Geochronol. St. Petersburg. 2009. P. 158-161.
6. Ustinov V.N., Zagainy A.K., Smith K.B., Ushkov V.V. Early Proterozoic diamondiferous kimberlites of Karelia and features of their formation // *Geology and geophysics*. 2009. T. 50. № 9. P. 963-977.
7. Ushkov V.V. Kimozero occurrence of diamondiferous kimberlites in the Onega structure // *Geology and minerals of Karelia*. 2001. № 3. P. 94-98.
8. Ushkov, V.V.; Ustinov, V.N.; Smith, C.B.; Bulanova, G.P.; Lukyanova, L.I.; Wiggers de Vries, D.; Pearson, D.G. Kimozero, Karelia; a diamondiferous Palaeoproterozoic metamorphosed volcanoclastic kimberlite /9IKC-A-00199.

**Gorbachev N.S., Kostyuk A.V., Nekrasov A.N., Soultanov D.M. Effect of carbonates Na and K on the phase composition and critical relation between carbonate and alcaic silicate melts in the eclogite-CaCO<sub>3</sub>-H<sub>2</sub>O+CO<sub>2</sub> system at P=4 GPa, T=1100-1400°C. UDC 550.4.02**

*Institute of Experimental Mineralogy RAS, Chernogolovka, Moscow district. (gor@iem.ac.ru, nastya@iem.ac.ru, alex@iem.ac.ru, dill@iem.ac.ru)*

**Abstract.** Influence of alkali carbonates on the phase relationships was studied in "dry" conditions and with H<sub>2</sub>O fluid in the eclogite-CaCO<sub>3</sub>-Na<sub>2</sub>CO<sub>3</sub>-K<sub>2</sub>CO<sub>3</sub> system at P=4 GPa, T=1100-1300°C. During melting of H<sub>2</sub>O-containing eclogite silicate melt is formed at T=1100°C, and immiscible silicate (L<sub>Sil</sub>) and carbonate (L<sub>Cb</sub>) melts coexisting with Cpx and Grt are formed at T=1200-1250°C. In the interval T 1250-1300°C there is a "critical" point T<sub>K</sub> of the equilibrium L<sub>Sil</sub>-L<sub>Cb</sub>, above which there is complete mixing between them. In the same system at P=4 GPa, T=1200°C in "dry" conditions, L<sub>Cb</sub> is formed as a result of liquation of the carbonatized silicate melt with the formation of immiscible L<sub>Sil</sub> and L<sub>Cb</sub> with Cpx on the liquidus.

*Keywords: eclogites, carbonates, chlorides, garnet, clinopyroxene, phase relations, melting, melts, mantle.*

Among the xenoliths of mantle rocks, along with peridotites, eclogites are found. In the nodules of mantle eclogites, the features of mantle metasomatism are widely manifested - the effect of supercritical fluids, carbonate melts and partial melting trails with the formation of phlogopite, apatite, carbonates and alkali enriched silicate glasses (up to 15 wt.%). The formation of alkaline and associated carbonatite magmas is associated with the melting of the metasomatically altered carbonatized upper mantle. As a rule, carbonatites occur in association with alkaline rocks of the Na series, much less often with enriched potassium (Na/K<1) rocks. The main components of metasomatic fluids and melts, along with H<sub>2</sub>O and CO<sub>2</sub>, are the salts (carbonates, chlorides) of Na and K. The effect of carbonates on phase ratios, silicate L<sub>Sil</sub> compositions and carbonate L<sub>Cb</sub> melts when melting eclogite in "dry" (without the addition of fluid) conditions, and also with H<sub>2</sub>O and CO<sub>2</sub> fluid was studied experimentally at P=4 GPa, T=1100-1300°C.

The experiments were carried out at the IEM RAS using a "anvil with hole" apparatus using a multi-ampoule quenching technique in Pt ampoules. The initial composition of the system is 70 wt.% of tholeiitic basalt, 30 wt.% of carbonates of Ca, Na and K. The composition of the carbonate is 90% of CaCO<sub>3</sub> (calcitic carbonate of Kovdor), carbonates Na<sub>2</sub>CO<sub>3</sub> - 5% and K<sub>2</sub>CO<sub>3</sub> - 5%, the ratio of oxides Na/K = 0.4. The source of the fluid was distilled water, its concentration ~ 10 wt. % relative to the silicate. The temperature was measured with a Pt30Rh/Pt6Rh thermocouple, the pressure was calibrated against the quartz-coesite equilibrium curve. The accuracy of determining the temperature and pressure in the experiments is estimated at ±5°C and ±1 kbar. The duration of the experiment was from 8 to 24 hours. The polished preparations of quenching samples were analyzed on an electronic scanning microscope with a secondary and reflected electron detector and an energy-dispersive spectrometer at the IEM RAS.

## The formation and differentiation of magmas

Effect of the temperature, fluid and composition of the system on the phase relationships and compositions of silicate and carbonate melts was revealed in eclogite systems.

At T=1100°C, the alkaline silicate melt coexisting with clinopyroxen (Cpx), garnet (Grt), and carbonate (Cb) is formed first during the melting of eclogite (Table 1).

At T increased up to 1200-1250°C, immiscible silicate and carbonate melts, Cpx and Grt are formed (Tables 2-3). The ratio of Na/K=0.3-0.5 in the silicate melt is close to the ratio in the initial mixture.

In the interval T=1250-1300°C there is a "critical" point  $T_k$  of equilibrium  $L_{Sil}$  and  $L_{Cb}$ , above which there is complete mixing between them (Table 3-4).

**Table 1. Chemical composition (wt.% oxides) of coexisting phases in the eclogite- $Na_2CO_3$ - $K_2CO_3$  +  $H_2O$  system at T=1100°C, P=4 GPa.**

	SiO <sub>2</sub>	TiO <sub>2</sub>	Al <sub>2</sub> O <sub>3</sub>	Cr <sub>2</sub> O <sub>3</sub>	FeO	MnO	MgO	CaO	Na <sub>2</sub> O	K <sub>2</sub> O	SrO	P <sub>2</sub> O <sub>5</sub>	Total
Grt	38.31	3.44	18.48	0.22	17.51	0.72	3.69	16.99	0.42	0.00	0.51	0.10	100.4
Cpx	50.51	0.90	3.28	0.60	9.41	0.33	13.33	19.21	0.51	0.04	0.96	0.40	99.48
Cb	0.08	0.11	0.04	0.00	0.97	0.14	0.62	47.98	0.00	0.06	0.62	0.04	50.66
Ap	0.74	0.00	0.15	0.25	0.98	0.05	0.36	49.27	0.45	0.14	0.93	38.75	92.07
$L_{Sil}$	55.56	0.42	16.62	0.03	0.51	0.00	0.06	0.30	2.88	10.36	0.51	0.27	87.53

**Table 2. The chemical composition (wt.% oxides) of coexisting phases in the eclogite- $Na_2CO_3$ - $K_2CO_3$  +  $H_2O$  system at T=1200°C, P=4 GPa.**

	SiO <sub>2</sub>	TiO <sub>2</sub>	Al <sub>2</sub> O <sub>3</sub>	Cr <sub>2</sub> O <sub>3</sub>	FeO	MnO	MgO	CaO	Na <sub>2</sub> O	K <sub>2</sub> O	SrO	P <sub>2</sub> O <sub>5</sub>	Total
Cpx	50.58	0.67	7.78	0.04	8.22	0.03	9.40	19.29	2.86	0.06	0.18	0.00	99.11
Cb	0.15	0.00	0.06	0.07	0.68	0.00	0.46	49.09	0.04	0.12	0.48	0.34	51.50
$L_{Sil}$	50.03	0.30	15.23	0.00	1.65	0.13	0.18	5.77	3.48	8.07	0.59	1.49	86.92
Bt	33.95	3.55	12.01	0.03	15.72	0.21	9.99	7.42	0.38	8.07	0.59	1.83	93.75
$L_{Cb}$	1.27	0.10	0.54	0.04	1.69	0.03	0.65	48.34	0.13	0.46	0.57	0.04	53.86
$L_{Cb}$	Si	44.04	0.62	12.94	0.00	2.39	0.14	0.48	7.76	1.78	7.67	0.31	79.86
	Cb	10.05	0.29	2.70	0.00	1.82	0.11	1.06	38.66	0.36	2.54	0.63	59.71

**Table 3. Chemical composition (wt.% oxides) of coexisting phases in the eclogite- $Na_2CO_3$ - $K_2CO_3$ + $H_2O$  system at T=1250°C, P=4 GPa.**

	SiO <sub>2</sub>	TiO <sub>2</sub>	Al <sub>2</sub> O <sub>3</sub>	Cr <sub>2</sub> O <sub>3</sub>	FeO	MnO	MgO	CaO	Na <sub>2</sub> O	K <sub>2</sub> O	SrO	P <sub>2</sub> O <sub>5</sub>	Total
Cpx	48.98	0.45	11.22	0.24	2.77	0.01	11.13	21.58	1.68	0.00	0.11	0.07	98.31
Cb	2.17	0.08	0.44	0.00	0.52	0.08	0.86	48.03	0.00	0.22	0.33	0.08	53.06
$L_{Sil}$	45.08	0.13	15.58	0.05	0.23	0.04	0.18	14.97	4.47	7.44	0.33	0.17	88.79
$L_{Cb}$	Si	42.56	2.19	9.58	0.01	4.28	0.02	10.47	21.13	1.60	0.12	0.44	95.13
	Cb	11.87	0.67	2.91	0.00	2.48	0.03	1.76	40.56	0.67	0.13	0.34	62.98

**Table 4. Chemical composition (wt.% oxides) of coexisting phases in the eclogite- $Na_2CO_3$ - $K_2CO_3$ + $H_2O$  system at T=1300°C, P=4 GPa.**

	SiO <sub>2</sub>	TiO <sub>2</sub>	Al <sub>2</sub> O <sub>3</sub>	Cr <sub>2</sub> O <sub>3</sub>	FeO	MnO	MgO	CaO	Na <sub>2</sub> O	K <sub>2</sub> O	SrO	P <sub>2</sub> O <sub>5</sub>	Total
CSFL	Si	35.80	1.67	8.32	0.00	9.50	0.45	4.53	25.25	2.81	0.50	1.33	91.29
	Cb	3.52	0.08	1.10	0.13	1.34	0.18	1.54	44.57	0.64	0.97	0.81	56.74
CSFL	21.62	1.15	5.61	0.00	5.37	0.20	4.90	34.35	1.09	1.48	0.73	1.84	78.69

**Table 5. Chemical composition (wt.% oxides) of coexisting phases in the eclogite-Na<sub>2</sub>CO<sub>3</sub>-K<sub>2</sub>CO<sub>3</sub> system at T=1200°C, P=4 GPa.**

	SiO <sub>2</sub>	TiO <sub>2</sub>	Al <sub>2</sub> O <sub>3</sub>	Cr <sub>2</sub> O <sub>3</sub>	FeO	MnO	MgO	CaO	Na <sub>2</sub> O	K <sub>2</sub> O	P <sub>2</sub> O <sub>5</sub>	Total
Chr	0.94	1.05	21.04	38.51	31.19	0.48	6.02	0.33	0.23	0.06	0.03	99.92
Cpx	51.37	0.47	9.40	2.68	6.53	0.23	9.12	14.16	4.73	0.17	0.00	98.93
L <sub>SiI</sub>	53.14	0.13	17.64	0.19	1.70	0.18	0.07	1.73	6.15	8.06	0.11	89.10
L <sub>Cb</sub>	1.62	0.04	0.73	0.14	12.09	0.71	1.18	21.98	14.08	1.44	0.44	54.71

In the same system, in "dry" conditions, carbonate melts are formed as a result of the liquation of the carbonatized silicate melt with the formation of immiscible silicate and carbonate liquids coexisting at T=1200°C with Cpx and chromite (Chr) relics.

Heterophase mixture of carbonate and silicate phases, apatite, and biotite is formed at quenching carbonate melts. In the diagrams of pairwise correlations of CaO-SiO<sub>2</sub>, the compositions of quenching phases of the carbonate melt form a linear trend, the extreme members of which are silicate Si and carbonate Cb components, isolated at the maximum concentrations of SiO<sub>2</sub> and CaO, respectively (Fig. 1).

A similar trend in the compositions of fluid-melt inclusions was observed in fibrous diamonds of Africa and Siberia. The existence of such a trend is considered as a sign of complete blending of the silicate and carbonatite components of the supercritical fluid melt.

Thus, at P = 4 GPa, the solidus temperature of the H<sub>2</sub>O-containing eclogite with carbonates Ca, Na, K ≤ 1150 ± 50 °C, liquidus temperature ≤ 1275 ± 25 °C. The subsolidus association is represented by Grt, Cpx, Cb. In partial melting, the first one at T = 1100 °C forms a high-K alkaline silicate melt coexisting with Cpx, Grt, Cb. With an increase in T and a degree of partial melting at T = 1200-1250 °C, the fraction (up to 10%) of the silicate melt increases, a carbonate melt appears, the main mineral of the liquidus is Cpx. The similarity of the Na/K ratio in silicate melts and in the initial charge indicates that the Na/K ratio in alkaline basalts, when formed, is determined by the Na/K ratio in the source. The immiscible L<sub>SiI</sub> and L<sub>Cb</sub> are stable in the range of T=1100-1250°C. In the interval T from 1250 to 1300°C there is a "critical" point of the T<sub>K</sub> equilibrium of alkaline silicate-carbonate melts, at the attainment of which complete mixing is observed between them. The critical temperature of the T<sub>K</sub> is 1275 ± 25°C. At T>T<sub>K</sub>, there is only one carbonatized silicate melt. During its quenching, a heterophase mixture of carbonate and silicate phases is formed, the compositions of which form a linear trend, the extreme members of which are silicate and carbonate components. Since alkaline chloride fluids are characteristic of subduction zones, the formation

of a multicomponent aggressive and mobile carbonate melt at TP parameters of the subducted plate can play an important role in the metasomatic transformation of the oceanic crust.

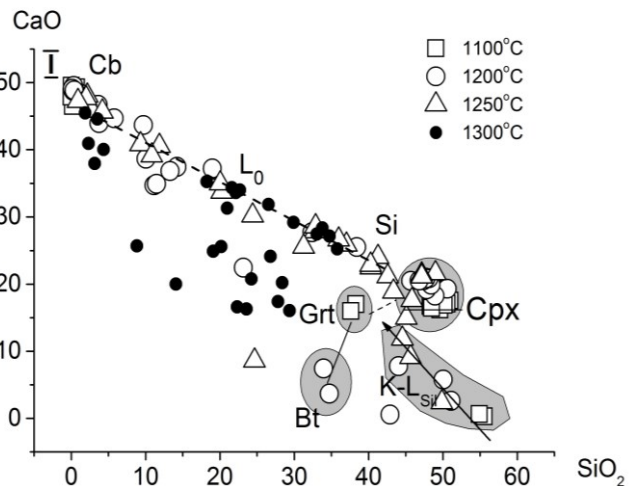


**Fig. 1.** The system of eclogite-Na<sub>2</sub>CO<sub>3</sub>-K<sub>2</sub>CO<sub>3</sub>+H<sub>2</sub>O. The composition of quenching samples in the coordinates of CaO-SiO<sub>2</sub> from experiments at P=4 GPa, T=1100, 1200, 1250 and 1300°C, showing the effect of T on the phase composition.

The work was supported by the RFBR grant 17-05-00930a.

**Gorbachev N.S., Kostyuk A.V., Nekrasov A.N., Soutanov D.M. Effect of chloride Na and K on the formation of undercritical carbonatites melts in the eclogite-CaCO<sub>3</sub>-H<sub>2</sub>O+CO<sub>2</sub> system at P=4 GPa, T=1200-1300°C. UDC50.4.02**

*Institute of Experimental Mineralogy RAS, Chernogolovka, Moscow district.* ([gor@iem.ac.ru](mailto:gor@iem.ac.ru), [nastya@iem.ac.ru](mailto:nastya@iem.ac.ru), [alex@iem.ac.ru](mailto:alex@iem.ac.ru), [dill@iem.ac.ru](mailto:dill@iem.ac.ru))

**Abstract.** The effect of alkali chlorides on the phase relationships in the eclogite-CaCO<sub>3</sub>-NaCl-KCl-H<sub>2</sub>O+CO<sub>2</sub> system was studied at P=4 GPa, T=1100-1300°C. The system is characterized by a narrow T interval between solidus (T<1200°C) and liquidus (T<1300°C) of eclogite. A fluid-containing high-Ca carbonate melt is formed throughout the T interval, coexisting in the subliquidus at T=1200-1250°C with Cpx and Grt. Heterophasic mixture of carbonate and silicate phases is formed during its quenching. In the CaO-SiO<sub>2</sub> diagram, their compositions

## The formation and differentiation of magmas

form a linear trend, the extreme members of which are the silicate and carbonate components, isolated at the maximum concentrations of SiO<sub>2</sub> and CaO. The existence of a carbonate melt in chlorine-containing eclogite systems at high pressures and low temperatures can play an important role in the mantle metasomatism of silicate rocks of the submerged subduction zone.

*Keywords: eclogites, carbonatites, chlorides, garnet, clinopyroxene, melting relations, melts, mantle.*

Among the xenoliths of mantle rocks, along with peridotites, eclogites are found. In the nodules of mantle eclogites, the features of mantle metasomatism are widely manifested - the effect of supercritical fluids, carbonate melts and partial melting tracks with the formation of phlogopite, apatite, carbonates and alkali enriched silicate glasses (up to 15wt.%). The main components of metasomatic fluids and melts, along with H<sub>2</sub>O and CO<sub>2</sub>, are Na and K salts (carbonates, chlorides). Interest in the study of mantle silicate systems with chlorine at high pressures is determined by the presence of chlorine in subduction fluids and their possible influence on phase ratios and the melting of rocks of the subducted Slab and mantle wedge (Uhanov et al., 1988; Pyle, Haggerty, 1998). Experimental studies of model systems with Cl have shown that the addition of chlorine to carbonate-silicate systems reduces the solidus temperature of carbonates, (Safonov et al., 2009; Litasov et al., 2010). There is also a wide range of immiscibility between chloride-carbonate and carbonate-silicate fluids, which decreases with increasing pressure and, possibly, disappears at pressures above 20 GPa. In the present work, the effect of alkali chlorides on the phase relationships and composition of the melts formed during the melting of the eclogite-CaCO<sub>3</sub>-NaCl-KCl system with H<sub>2</sub>O+CO<sub>2</sub> by the fluid at P=4GPa was studied in the interval T=1200-1300°C.

The experiments were carried out at the IEM RAS at the "anvil with hole" apparatus in Au and Au-

Pd ampoules using a multi-ampoule technique (Gorbachev, 1989). Starting materials: tholeiitic basalt, chemical analogue of the average Siberian trap, calcitic carbonate of Kovdor, NaCl, KCl, oxalic acid dihydrate H<sub>2</sub>C<sub>2</sub>O<sub>4</sub>·2H<sub>2</sub>O as source of H<sub>2</sub>O+CO<sub>2</sub> fluid. The initial concentration of CaCO<sub>3</sub> is 40 wt. %, H<sub>2</sub>C<sub>2</sub>O<sub>4</sub>·2H<sub>2</sub>O, NaCl + KCl - 10 wt. % With respect to silicate, Na/K ratio in chloride 0.76. The temperature was measured by a Pt30Rh/ Pt6Rh thermocouple, the pressure at high temperatures was calibrated along the quartz-coesite equilibrium curve. The accuracy of determining the temperature and pressure in the experiments is estimated at ±5°C and ±1 kbar (Litvin, 1991). The duration of the experiment was from 8 to 24 hours. After quenching, the ampoule was sawn in the longitudinal direction, then its parts in a special mold under pressure and heating were pressed into polystyrene. From the resulting tablet in a "dry" conditions, polished preparations were prepared. Their peculiarity was the formation of a film consisting of microcrystals of Na and K chlorides during the first day on the surface of the sample, indicating the decomposition and degassing of hardening products of alkaline Cl-H<sub>2</sub>O-CO<sub>2</sub>-containing carbonate melt (CSFL). Polished tablets were studied and analyzed on an electronic scanning microscope TESCAN VEGA II XMU equipped with a secondary and reflected electron detector and an INCA Energy 450 energy dispersive spectrometer and an INCA WEVE wave dispersion spectrometer at the IEM RAS.

The texture and phase relationships of quenching samples depend on temperature (Table 1, Fig.1-4).

At T=1200°C, P=4 GPa, quenching samples are characterized by a "massive" texture. They are composed of clinopyroxene (Cpx), garnet (Grt), carbonateCb (Fig. 1).

**Table 1. Representative chemical composition (in wt.% of oxides) of coexisting phases in the eclogite-NaCl-KCl + H<sub>2</sub>O+CO<sub>2</sub> system at T=1200-1300°C, P=4 GPa.**

	SiO <sub>2</sub>	TiO <sub>2</sub>	Al <sub>2</sub> O <sub>3</sub>	FeO	MnO	MgO	CaO	Na <sub>2</sub> O	K <sub>2</sub> O	Cr <sub>2</sub> O <sub>3</sub>	P <sub>2</sub> O <sub>5</sub>	Total
T = 1200°C												
Cpx	49.92	0.07	11.37	1.73	-	12.81	22.56	1.40	0.02	0.14	-	100.02
Grt	39.19	0.49	22.31	6.76	0.18	9.45	21.01	0.20	0.00	0.16	-	99.75
Cb	0.00	0.00	0.27	0.92	0.21	3.35	46.96	0.00	0.08	0.00	-	51.79
T = 1250°C												
Cpx	47.38	0.31	13.05	1.04	0.02	11.77	23.91	0.89	0.00	0.31	0.00	98.68
Grt	39.91	0.25	21.87	3.38	0.00	8.14	25.32	0.21	0.04	0.29	0.03	99.44
Ap	1.40	0.02	0.22	0.25	0.14	1.92	50.79	1.59	0.32	0.05	30.39	87.09
L <sub>Cb</sub>	9.30	0.30	2.99	0.47	0.05	4.68	39.63	0.48	0.81	0.00	2.63	61.35
T = 1300°C												
CSFL	14.88	0.65	5.23	1.78	0.26	6.59	42.02	0.60	1.27	0.00	2.95	76.22

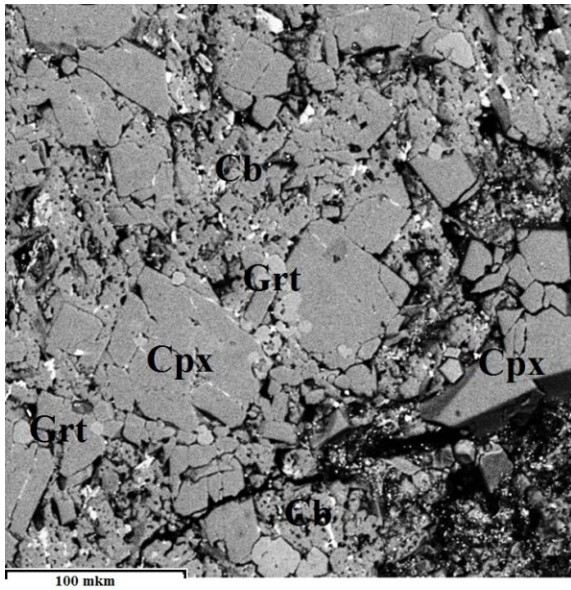


**Fig. 1.** Microphotographs of experimental samples in secondary electrons, characterizing the texture and phase composition in the eclogite-NaCl-KCl-H<sub>2</sub>O + CO<sub>2</sub> system at T = 1200 °C.

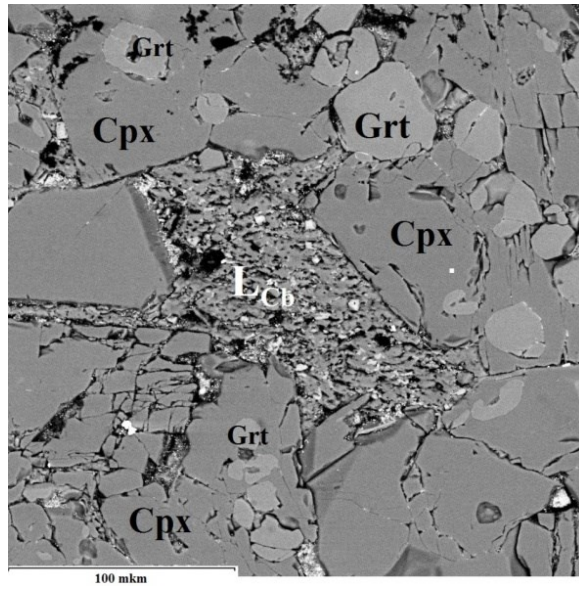


**Fig. 2.** Microphotographs of experimental samples in secondary electrons, characterizing the texture and phase composition in the eclogite-NaCl-KCl-H<sub>2</sub>O + CO<sub>2</sub> system at T=1250°C.

Cpx composition  $\text{Na}_{0.1}\text{Ca}_{0.83}\text{Mg}_{0.66}\text{Fe}_{0.05}\text{Al}_{0.46}\text{Si}_{1.72}\text{O}_6$  in the form of tabular crystals, up to 50 microns in size, predominates among the silicate phases. The content of Ca and Mg is close to that of diopside, characterized by a high content of alumina (up to 11 wt.%  $\text{Al}_2\text{O}_3$ ) and Na (up to 1.4 wt.%  $\text{Na}_2\text{O}$ ). Grt grossular-pyropes-almandine composition  $\text{Ca}_{1.67}\text{Mg}_{1.04}\text{Fe}_{0.42}\text{Al}_{1.95}\text{Ti}_{0.03}\text{Si}_{2.90}\text{O}_{12}$  occurs as an oval form of inclusions on contact with Cpx, and also forms microinclusions in it. By the ratio of  $\text{Cr}_2\text{O}_3$ -CaO corresponds to eclogite paragenesis (Sobolev, 1974). Calcite carbonate, microporous, with an admixture of Mg oxides (up to 4 wt.%), Fe, Na, K, Si, Al (up to 1 wt.%) cement Cpx and Grt. The volatile content is about 48 wt. %.

The absence of silicate glass, a characteristic feature of the existence of a silicate melt, indicates that the temperature of the solidus ( $T_C$ ) of eclogite in this system is above 1200°C. At the same time, the composition and structure of the carbonate, its relationship with Cpx and Grt, suggest that Cb is a quenching product of a carbonate melt. The formation of a high-Ca carbonate melt in the subsolidus of the eclogite can be explained by the existence of a low-temperature ( $\leq 700^\circ\text{C}$ ) eutectic in the NaCl-KCl-CaCO<sub>3</sub> system (Jones, 2013).

The low contents of Fe, Si, Al components in Cpx and Grt can be explained by the low solubility of these minerals in the carbonate melt, and Na, K, Cl - their loss upon its decomposition and degassing. When the temperature is raised to 1250°C, the quenching samples are represented by the liquidus association Cpx + Grt, which is similar in composition to Cpx and Grt of the subsolidus and

isolated regions consisting of a heterophase fine-dispersed mixture of carbonate and silicate phases, apatite, Na and K chlorides, and carbonate melt quenching products. Silicate glass was not observed. Tabular segregations Cpx of composition  $\text{Na}_{0.06}\text{Ca}_{0.9}\text{Mg}_{0.62}\text{Fe}_{0.03}\text{Al}_{0.54}\text{Si}_{1.68}\text{O}_6$  contain an oval form of inclusion Grt, composition  $\text{Ca}_{2.01}\text{Mg}_{0.9}\text{Fe}_{0.21}\text{Al}_{1.91}\text{Ti}_{0.01}\text{Si}_{2.95}\text{O}_{12}$ , which also forms independent precipitates (Fig. 2).

At T=1300°C quenching samples are represented by a heterophase mixture of carbonate and silicate phases, apatite, Na chloride, formed during quenching of the carbonate melt (Fig. 3).

The absence of liquidus minerals and silicate glass, the texture and composition of the quench phases, characteristic of quenching carbonate melt, indicate the under-liquidus experimental conditions and complete mixing of silicate and carbonate melts with the formation of a supercritical carbonatite melt. Therefore, at P=4 GPa, the critical temperature  $T_K$  of carbonatite melt-alkaline silicate melt equilibrium is about  $1250^\circ\text{C} < T_K < 1250^\circ\text{C}$ . In the diagrams of pairwise correlations of CaO-SiO<sub>2</sub>, the compositions of quenching phases of the carbonate melt form a linear trend, the extreme members of which are silicate Si and carbonate Cb components, isolated at the maximum concentrations of SiO<sub>2</sub> and CaO, respectively. The composition of the coexisting phases in the eclogite-NaCl-KCl-H<sub>2</sub>O+CO<sub>2</sub> system in the coordinates of CaO-SiO<sub>2</sub> at T=1200-1300°C, P=4 GPa is shown in Fig.4.

Thus, in the eclogite-CaCO<sub>3</sub>-chlorides of alkalis with H<sub>2</sub>O+CO<sub>2</sub> fluid in the interval T=1200-1250°C, the carbonate melt coexists with Cpx and Grt. The

oval form of Grt and the presence of its relics in Cpx indicate the reaction ratios of Grt to the carbonate melt and Cpx. At  $T=1300^{\circ}\text{C}$  there is only a supercritical carbonate melt. The narrow ( $\leq 100^{\circ}\text{C}$ )  $T$  interval between the solidus ( $T>1200^{\circ}\text{C}$ ) and the liquidus ( $T<1300^{\circ}\text{C}$ ) of eclogite is characteristic for the near-eutectic compositions. The existence of an alkaline fluid-chloride-carbonate melt in chlorine-

containing eclogite systems at high pressures and low temperatures can play an important role in mantle metasomatism. Particularly interesting in this respect are the subduction zones with a characteristic water-alkaline-chloride type of fluids in which low-temperature chlorine-containing carbonate melts can exist even for PT cold-subduction conditions in the subsolidus of silicate rocks of the subduction slab.

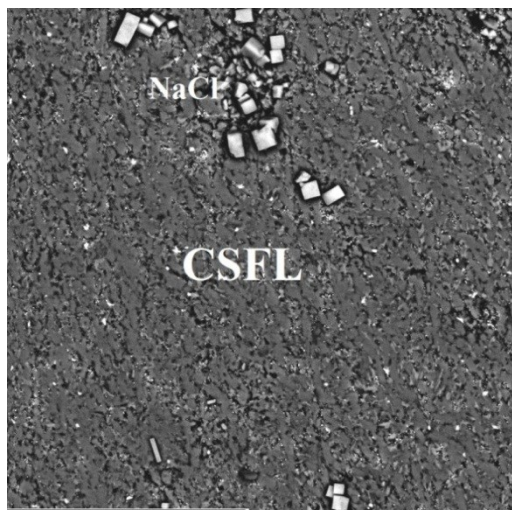


**Fig. 3.** Microphotographs of experimental samples in secondary electrons, characterizing the texture and phase composition in the eclogite-NaCl-KCl-H<sub>2</sub>O + CO<sub>2</sub> system at  $T=1300^{\circ}\text{C}$ .

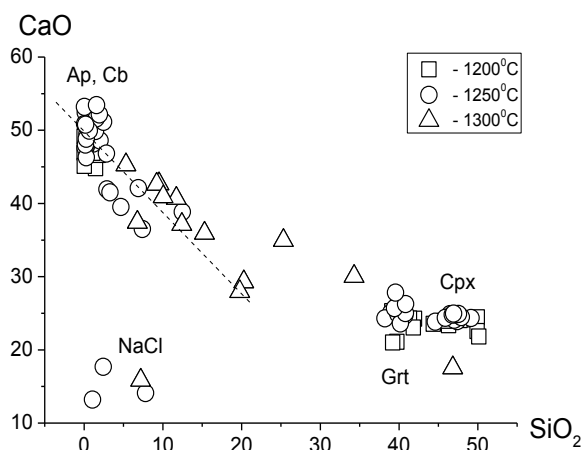


**Fig. 4.** Composition of coexisting phases in the eclogite-NaCl-KCl-H<sub>2</sub>O+CO<sub>2</sub> system in the coordinates of CaO-SiO<sub>2</sub> at  $T=1200-1300^{\circ}\text{C}$ ,  $P=4\text{GPa}$ .

The work was supported by the RFBR grant 17-05-00930a.

### References:

1. Gorbachev N.S. Fluid-magmatic interaction in sulphide-silicate systems. 1989. M. Nauka. Litasov K.D., Sharygin I.S., Shatsky A.F. and others. DAN. 2010. v.435. №5. P.667-672. LitvinYu.A. Physicochemical studies of the melting of the Earth's deep matter. 1991. M. Nauka. Safonov O.G., Perchuk L.L., Yapaskurt V.O., and others. DAN. 2009. T.424. No. 3. P. 388-392. Sobolev N.V. Deep inclusions in kimberlites and the problem of the composition of the upper mantle. Nauka. Novosibirsk, 1974. P. 264
2. Ukhanov A.V., Ryabchikov I.D., Kharkiv A.D. Lithospheric mantle of the Yakut kimberlite province. 1988. M. Nauka. C.286.
3. A.P. Jones, M. Genge, L. Carmody. Reviews in Mineralogy and Geochemistry. 2013. V. 75. p. 289-322.
4. Pyle, J.M., Haggerty, S.E. Geochim Cosmochim Acta, 1998, V.62, p.1207-1231.

**Gorbachev N.S., Kostyuk A.V. Experimental investigations of melting of fluid-containing upper mantle at subcritical and supercritical P-T conditions with the use of multi-ampoule methodology with peridotite ampoule. UDC 550.4.02**

*Institute of Experimental Mineralogy RAS, Chernogolovka, Moscow district. ([gor@iem.ac.ru](mailto:gor@iem.ac.ru), [nastya@iem.ac.ru](mailto:nastya@iem.ac.ru))*

**Abstract.** The existence of critical relationships between silicate melts and aqueous fluid at high P-T is a feature of fluid-containing silicate systems. Platinum and peridotite ampoules, basalt and fluid are proposed to be used to fix the transition from subcritical to supercritical state. Features of the texture and phase composition of quenching samples are an indicator of such a transition. At subcritical P-T inter-grain silicate glass cemented peridotite ampoule and fills its internal part. The absence of intergranular melt in supercritical P-T leads to destruction of peridotite ampoule consisting of relict minerals, quenching products of supercritical fluid melt and reaction phases formed during the interaction of supercritical fluid melt with restite minerals. The complete disintegration of the quench sample, wholly consisting of quenching products of the supercritical fluid melt, is observed at P-T at the second critical endpoint.

**Keywords:** *experiment, melting relations, melts, mantle, fluid, critical relations.*

A feature of fluid-containing silicate systems is the existence of critical relationships between silicate melts and aqueous fluid, due to their high mutual solubility. Full miscibility is observed between the melt and the fluid at supercritical pressures ( $P_k$ ) and temperatures ( $T_k$ ). At the second final critical point ( $2P_kT_k$ ), when the P-T solidus of the silicate and  $P_k$  and  $T_k$  of the two-phase melt-fluid equilibrium is

equal, the full miscibility is observed between liquidus phases, melt and fluid, which makes it difficult to determine the solidus. In most experimental studies, "remote" research methods were used, without material analysis, in which the transition from subcritical to supercritical state was detected optically in hydrothermal diamond anvils (Shen, Keppler, 1997), using high-temperature X-ray radiography (Mibe et al. 2007). The possibilities of the first method are limited to model silicate systems with low T solidus, such as Ab, Ne, Jd, dacite, haplogranite (Bureau, Keppler, 1999). The only exception is the work on the study of critical ratios in the SiO<sub>2</sub>-H<sub>2</sub>O system, SiO<sub>2</sub>-MgO-H<sub>2</sub>O, eclogite-H<sub>2</sub>O, peridotite-basalt-H<sub>2</sub>O using the quenching method, which analyzed the composition of matter, pre- and supercritical fluid, silicate phases (Kennedy et Al., 1962, Stalder et al., 2001, Kessel et al., 2005, Gorbachev, 2000).

To fix the transition of the peridotite-fluid system from the subcritical to the supercritical state, we propose to use an experimental ensemble consisting of platinum and peridotite ampoules and the initial charge. Peridotite ampoule, prepared by forming and sintering peridotite, is filled with the initial charge consisting of basalt, fluid source, accessory minerals, placed in Pt ampoule, which is hermetically sealed. Polished samples were studied and analyzed on a microprobe.

*Subcritical P-T conditions.* With partial melting of peridotite, the original structure of the sample was preserved by the peridotite ampoule, filled with silicate glass, the product of quenching of the basaltic

melt. Quenching samples are characterized by a massive structure due to the fact that during partial melting, intergranular silicate glass is quenching silicate melt, cement the peridotite ampoule and fill its inner part. Under the experimental conditions, the phase composition is represented by the equilibrium association of peridotite restite and melt. The formation of quenching phases, immiscible melts (sulfide, carbonate) does not change the massive structure of the sample. In the peridotite (ampoule) - basalt-sulphide-H<sub>2</sub>O+CO<sub>2</sub> system, subcritical conditions are preserved up to T=1450°C, P=4GPa, and in experiments with H<sub>2</sub>O fluid to T=1400°C, P=2.5 GPa (Gorbachev et al., 2008). The structures and phase relationships of quenching samples are shown in Fig. 1.

*Supercritical P-T conditions.* At critical P-T of the melt-fluid equilibrium the quench glass is not formed. The absence of intergranular melt leads to the destruction of the peridotite ampoule, consisting of isolated liquidus minerals - olivine, ortho- and clinopyroxenes. Its internal part consists of quenching products of supercritical fluid melt in the form of a loose, unbound mixture of silicate microlites, sulfide and aluminosilicate microglobules, reaction phases formed during the interaction of supercritical fluid melt with minerals of restite peridotite. In Fig. 2 shows photomicrographs of the experimental sample characterizing the structure and phase composition in the peridotite (ampoule)-basalt-sulfide-alkaline-water-carbonate fluid system at 1400°C, 4GPa (Gorbachev et al., 2008).

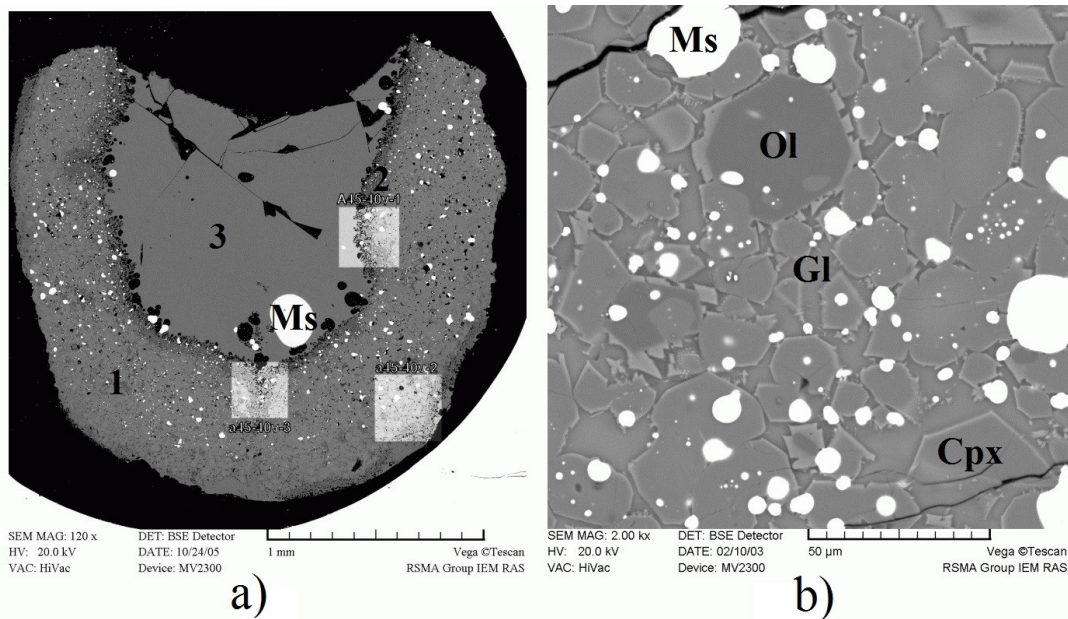


**Fig. 1.** Peridotite-basalt-H<sub>2</sub>O system, T=1400°C, P=2.5 GPa. A micrograph of quenching samples in secondary electrons at subcritical P-T: a) peridotite ampoule, general view: 1-peridotite ampoule; 2-reaction zone; 3-silicate glass, b) the texture and phase composition of the peridotite ampoule.

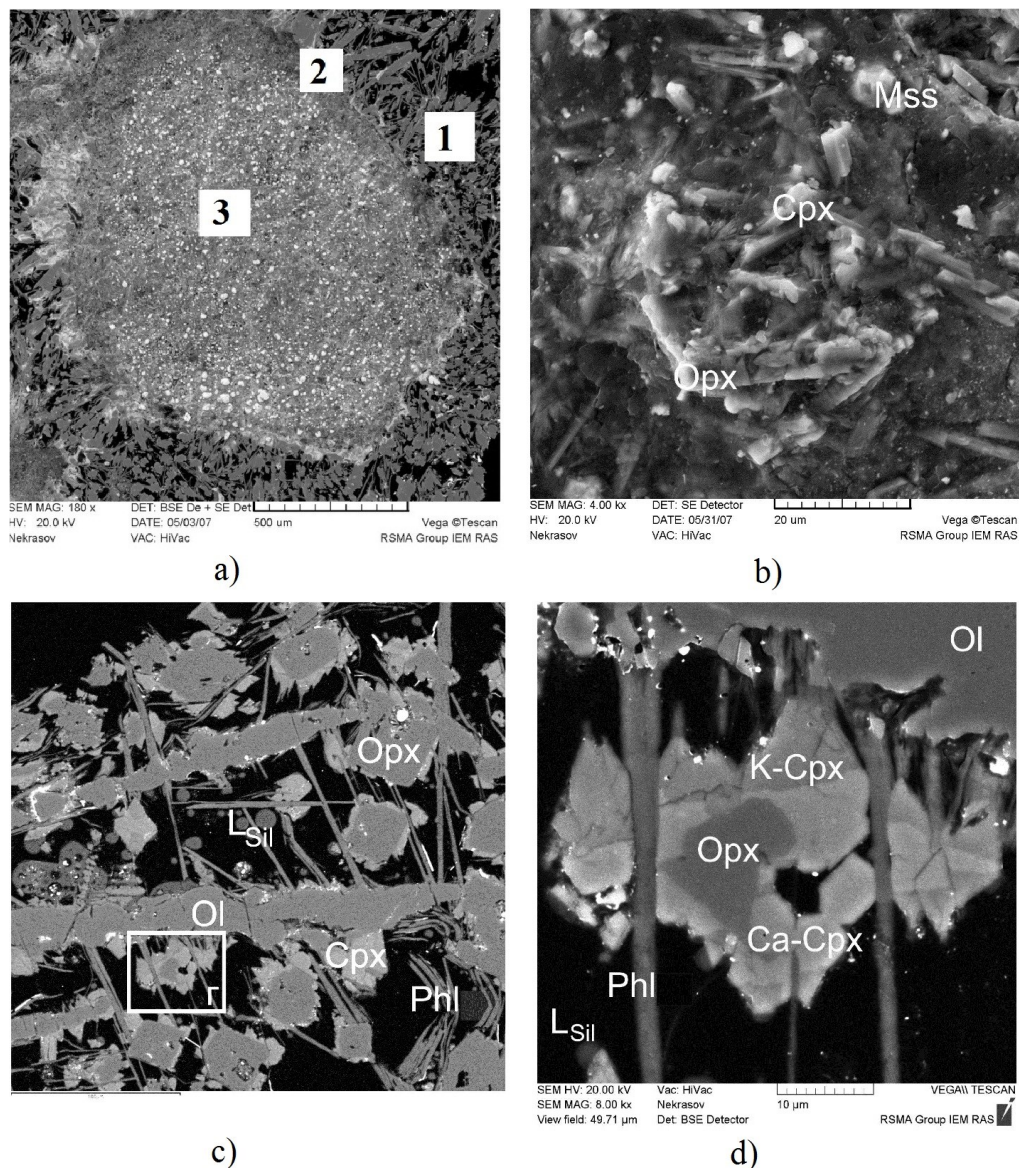


**Fig. 2. Peridotite-basalt- (K, Na)<sub>2</sub>CO<sub>3</sub>-H<sub>2</sub>O system, T=1400°C, P=4.0GPa. Microphotographs of quenching sample (Gorbachev et al., 2008) a) longitudinal section of ampoule: 1 - peridotite ampoule ; 2 - reaction zone at the peridotite-basalt contact; 3 - internal, basalt part; b) microlites of the quench supercritical fluid melt of the basalt part; c) the reaction ratio Ol-Opx-CaCpx-KCpx-carbonate-phlogopite in the interaction of supercritical fluid melt with minerals of restite peridotite; d) phase relations of Fig. 2c, marked with a square.**



**Fig. 3. Peridotite-basalt-H<sub>2</sub>O system at T=1400°C, P=4.0 GPa, close to the final critical point (Gorbachev, 2000). Microphotographs of the quenching sample in reflected electrons. Form of excretions of quenching material of supercritical fluid melt.**

The interaction of Ol-Opx-CaCpx-KCpx-carbonate, the formation of phlogopite, and the quenching of supercritical fluid melt form the Al-Si globule are associated with the interaction of the supercritical fluid melt with the minerals of restite peridotite. Absence of signs of partial melting, anomalous phase composition and structure of samples, dissolution of relict minerals of peridotite, formation of reaction fringes, hardening phases indicate melting of peridotite under supercritical conditions, and reaction relationships indicate high reactivity of supercritical fluids.

In the peridotite (ampoule)-basalt-sulfide-H<sub>2</sub>O system at T=1400°C, P=4 GPa, complete disintegration of quenching samples consisting of an unrelated mixture of microlites of silicate minerals and their intergrowths of needle, dendritic form, with globules of silicate glass, sulphides (Gorbachev,

2000). The disintegration of the samples, the absence of signs of partial melting-the intergranular melt, the liquidus association, indicate critical ratios in the system at P and T close to the final critical point (Fig. 3).

Thus, the proposed technique can serve as a test for the transition of fluid-containing peridotite systems from subcritical to supercritical state and determine the PT transition. In addition, the proposed technique makes it possible to study the features of the phase composition during the partial melting of the fluid-containing peridotite at pre- and supercritical P-T, the interaction of supercritical fluids with peridotite minerals.

The work was supported by the RFBR grant 17-05-00930a.

References:

1. Gorbachev N.S. The supercritical state in the water-containing mantle (according to the experimental study of the fluid containing peridotite at P = 40 kbar, T = 1400°C) // DAN. 2000. 371.3. Pp. 362-365.
2. Gorbachev NS, Kostyuk AV, Nekrsov AN Partial melting of fluid peridotite under subcritical and supercritical P-T conditions: textural and mineralogical differences. Vestnik of the ONZ RAS. №1, 2008. URL: [http://www.scgis.ru/russian/cp1251/h\\_dggms/1-2008/informbul-1\\_2008/magm-8.pdf](http://www.scgis.ru/russian/cp1251/h_dggms/1-2008/informbul-1_2008/magm-8.pdf)
3. H. Bureau, H. Keppler. Complete miscibility between silicate melts and hydrous fluids in the upper mantle: experimental evidence and geochemical implications // Earth Planet Sci. Lett. 1999. 165. p.187-196.
4. Kennedy G.C., Wasserburg G.J., Heard H.C., Newton R.C. The upper three-phase region in the system SiO<sub>2</sub>-H<sub>2</sub>O // Am J Sci. 1962. 260(7):501-521.
5. Mibe K., Kanzaki M., Kawamoto T., Matsukage K. N., Fei Y. and Ono S. Second critical endpoint in the peridotite-H<sub>2</sub>O system // J. Geophys. Res. 2007. 112, B03201.
6. R. Kessel, P. Ulmer, T. Pettke, M.W. Schmidt, A.B. Thompson. The water-basalt system at 4 to 6 GPa: Phase relations and second critical endpoint in a K-free eclogite at 700 to 1400°C // Earth and Planetary Science Letters, 2005. V. 237. P. 873-892.
7. Shen A.H., Keppler H. Direct observation of complete miscibility in the albite-H<sub>2</sub>O system // Nature. 1997. 386(6618):710-712.
8. Stalder R., Ulmer P., Thompson A.B., Gunther D. High pressure fluids in the system MgO-SiO<sub>2</sub>-H<sub>2</sub>O under upper mantle conditions // Contrib. Mineral. Petrol. 2001. V.140. P. 607-618.

**Kotelnikov A.R.<sup>1</sup>, Suk N.I.<sup>1</sup>, Korzhinskaya V.S.<sup>1</sup>, Kotelnikova Z.A.<sup>2</sup>, Shapovalov Yu.B.<sup>1</sup>**  
**Investigation of rear and rare-earth ore components distribution in the systems**

**aluminosilicate melt – fluoride salt melt at T=800-1200°C and P=2 kbar (in water presence).**

<sup>1</sup>Institute of Experimental Mineralogy RAS, Chernogolovka Moscow district, <sup>2</sup>*Institute of Geology of Ore Deposits, Petrography, Mineralogy, and Geochemistry, RAS* (kotelnik@iem.ac.ru, [sukni@iem.ac.ru](mailto:sukni@iem.ac.ru), vkor@iem.ac.ru, kotelnik@igem.ru, shap@iem.ac.ru)

**Abstract.** Melting in the system aluminosilicate (granitic) melt – fluoride salt melt has been experimental investigated at T=800-1200°C and P=2 kbar. The trituration of granite (Orlovka, hole 42) previously melting at 1200°C and 4 kbar during 6 h, NaF, oxides of REE (La, Ce, Y, Gd, Dy) or Nb, Ta, Ti or Zr, Hf, V were used as starting material. Experiments were produced in high gas pressure vessel with duration from 1 to 5 days depending on P-T parameters. Data of phase composition of silicate-salt systems and ore components partition coefficients are presented.

*Keywords: experiment, melt, liquid immiscibility, fluoride, partition coefficients*

Melting in the system aluminosilicate (granitic) melt – fluoride salt melt has been experimental investigated at T=800-1200°C and P=2 kbar. The purposes of this investigation were: (1) study of phase equilibria in fluid-magmatic system in presence of sodium fluoride and water (at T=800, 900 and 1200°C; P=1-2 kbar); (2) estimation of phase distribution of ore elements (Ti, Zr, Hf; V, Nb, Ta; Y, La, Ce, Gd, Dy) in fluoride-bearing fluid-magmatic system at these PT-parameters.

**Experimental method**

The powder of granite (Orlovka, hole 42) preliminary melting at 1200°C, 4 kbar during 6 h and NaF were used as starting materials. Granite glass composition is (mass.%): SiO<sub>2</sub> – 72.1; TiO<sub>2</sub> – 0.01; Al<sub>2</sub>O<sub>3</sub> – 16.14; Fe<sub>2</sub>O<sub>3</sub> – 0.68; MnO – 0.09; CaO – 0.3; MgO – 0.01; Na<sub>2</sub>O – 5.17; K<sub>2</sub>O – 4.28; P<sub>2</sub>O<sub>5</sub> – 0.02; ignition loss – 0.95; Σ=99.75; H<sub>2</sub>O – 0.18; F – 0.32. Glass composition calculated by CIPW method to norm content is (mass.%): Qz 25.6; Cd – 3.0; Ort – 25.3; Ab – 43.7; Hyp – 0.02; Mt – 0.3; Hem – 0.5; Ilm – 0.02; Ap – 0.05; Fl – 0.40. Webster parameters for this granite are following: A/CNK=1.159; X<sub>Al</sub><sup>Melt</sup>=0.209; K<sub>agg</sub>= 0.81; C/S =0.0044; X<sub>K</sub><sup>Melt</sup> = 0.345. As ore components some quantity of REE oxides (La, Ce, Y, Gd, Dy) or Nb, Ta, Ti, or Zr, Hf, V (1 mg of each component) has been loaded to the charge. Two types of charge were used: (1) most part of experiments has been produced used initial mixture: 50 mg of granite glass + 5 mg NaF + 5 mg H<sub>2</sub>O + (3-5) mg of ore elements oxides; (2) a part of experiments at 1200°C has been produced used starting composition: 40 mg of granite glass + 20 mg NaF + 6 mg H<sub>2</sub>O + (3-5) mg of ore elements oxides. Experiments have been produced in high gas pressure vessel at different regimes: 1) primary

## The formation and differentiation of magmas

melting (1 hour) at T=1250°C, P=5 kbar and then parameters were reduced to necessary conditions with run time during 5 hours; (2) at necessary parameters during 1 day. Experimental products have been analyzed by microprobe method.

### Phase composition of experimental products

**At T=800°C** silicate glass with F content up to 2.5 mass. %, little drops of fluoride phase and crystal phase with composition which depends on the charge of ore components are presented in experimental products. With REE in the charge silicates of REE form, with TiO<sub>2</sub>, ZrO<sub>2</sub> and HfO<sub>2</sub> in the charge crystals of zircon, baddeleyite and gadolinite are obtained, with V<sub>2</sub>O<sub>5</sub>, Nb<sub>2</sub>O<sub>5</sub>, Ta<sub>2</sub>O<sub>5</sub> in the charge pyrochlore-microlite synthesizes. Its formula calculated for 4 cations is following: (Na<sub>0.72</sub>K<sub>0.10</sub>Ca<sub>0.92</sub>)<sub>1.74</sub>(V<sub>0.10</sub>Nb<sub>1.33</sub>Ta<sub>0.82</sub>)<sub>2.25</sub>O<sub>6</sub>[F<sub>0.41</sub>(OH)<sub>1.5</sub>]<sub>1.91</sub>. Phase compositions are presented in table 1.

**At T=900°C** in experiments with REE phase composition is presented by silicate glass (F – 2.45 mass. % at P=1 kbar and F – 1.57 mass.% at P=2

kbar) and fluoride melting phases most often with following composition: (NaF)<sub>0.21</sub>Cry<sub>0.20</sub>Flu<sub>0.05</sub>[(REE)F<sub>3</sub>]<sub>0.54</sub>, where Cry – cryolite (Na<sub>3</sub>AlF<sub>6</sub>), Flu – fluorite (CaF<sub>2</sub>). At 900°C and P=1-2 kbar this phase is presented by melt coexisting with aluminosilicate melt. Some crystals with composition of (REE)F<sub>3</sub> are presented, too. In experiments with V, Nb, and Ta in the charge only fluoride-bearing glass (F ≤ 1.0 mass. %) at P=1 kbar, or glass without F at P=2 kbar and cryolite crystals are obtained.

In experiments with Ti, Zr and Hf in the charge silicate glass with low F content (F – 0.8 mass. % at P=1 kbar and F – 0.2 mass. % at P=2 kbar) and melting fluoride phase consist of mixture of NaF, cryolite and some amount of fluorite which does not contain elements of this group are presented. It should be noted that at 900°C agpaitic coefficient (K<sub>agp</sub>) of granite glass increases from 1.74 (charge with REE) to 1.85 (charge with

**Table 1. Phase compositions of experimental products at T= 800, 900 and 1200°C and P=1-2 kbar**

P, kbar	Charge	Phase compositions of experimental products
T=800°C		
1	(1) (Y,...Dy)	Silicate glass (F) <sup>1)</sup> + fluoride drops + REE silicate crystals
1	(1) (V, Nb,Ta)	Silicate glass (F)+ fluoride drops + crystals of pyrochlore
1	(1) (Ti, Zr, Hf)	Silicate glass (F) + crystals of zircon, baddeleyite, gadolinite
T=900°C		
1	(1) (Y,...Dy)	Silicate glass (F) + fluoride drops + crystals of cryolite(?)
1	(1) (V, Nb,Ta)	Silicate glass (F) + cryolite
1	(1) (Ti, Zr, Hf)	Silicate glass (F) + fluoride drops
2	(1) (Y,...Dy)	Silicate glass (F) + fluoride drops
2	(1) (V, Nb,Ta)	Silicate glass (F) + cryolite
2	(1) (Ti, Zr, Hf)	Silicate glass (F) + fluoride drops
T=1200°C		
1	(1) (Y,...Dy)	Silicate glass (F) + fluoride drops
1	(1) (V, Nb,Ta)	Silicate glass (F)
1	(1) (Ti, Zr, Hf)	Silicate glass (F)
2	(1) (Y,...Dy)	Silicate glass (F) + fluoride drops
2	(1) (V, Nb,Ta)	Silicate glass (F) + fluoride drops
2	(1) (Ti, Zr, Hf)	Silicate glass (F)
2	(2) (Y,...Dy)	Silicate glass (F) + fluoride drops + crystals of fluorides
2	(2) (V, Nb,Ta)	Silicate glass (F) + fluoride drops + crystals of fluorides
2	(2) (Ti, Zr, Hf)	Silicate glass (F) + crystals of fluorides

1) Silicate glass (F) – fluoride-bearing glass of granite composition; fluoride drops – drops of NaF.

V, Nb and Ta) and up to 1.94 (charge with Ti, Zr and Hf) and F content decreases from 2.45 mass.% (charge with REE) to 0.76 mass.% (charge with Ti, Zr and Hf) at P=1 kbar. Analogical behaviour is observed at P=2 kbar: K<sub>agp</sub> increases from 1.66

(charge with REE) to 1.94 (charge with Ti, Zr and Hf) respectively and F content in glass decreases from 1.57 to 0.23 mass. %.

So, in experiments at 900°C inverse correlation of apgaitic coefficient of aluminosilicate glass and F content in it takes place.

At 1200°C in experiments with charge 1 two melting phases (aluminosilicate melt and fluoride melt containing REE) have formed and in experiments with V, Nb, Ta and Ti, Zr, Hf only aluminosilicate melt with high content of F – 3.9-4.2 mass. % is present. At 2 kbar in experiments with REE and with V, Nb, Ta two melting phases (aluminosilicate melt and fluoride melt) are observed and in experiments with Ti, Zr, Hf one aluminosilicate melt with relative high F concentration (3.83 mass. %) is observed. In experiments with high starting F concentration (charge 2) with REE and with V, Nb, Ta three melting phases (aluminosilicate melt, fluoride drops containing ore elements and drops of pure NaF) form; in experiments with Ti, Zr, Hf aluminosilicate melt and drops of NaF form. At 1200°C (charge 1) it is observed analogical with experiments at 900°C behaviour:  $K_{\text{agp}}$  increases from 1.25 (charge with REE) to 1.57 (charge with Ti, Zr, Hf) at P=1 kbar and from 1.13 (charge with REE) to 1.54 (charge with Ti, Zr, Hf) at P=2 kbar. But F behaves differently: in experiments positive correlation between F content and melt alkalinity ( $K_{\text{agp}}$ ) has been estimated: at P=1 kbar  $K_{\text{agp}}$  increases from 1.25 (charge with REE) to 1.57 (charge with Ti, Zr, Hf) and F concentration increases from 1.70 mass.% (charge with REE) to 3.90 mass.% (charge with Ti, Zr, Hf). Analogical behaviour is observed at pressure elevation up to 2 kbar, too. At once used charge 2 we have obtained following results in experiments at 1200°C: apgaitic coefficient increases from 1.63 (charge with REE) to 1.86 (charge with Ti, Zr, Hf) and F content in glass decreases from 1.60 mass. % (charge with REE) to 1 mass.% (charge with Ti, Zr, Hf). Such variations of glass compositions in presence F-bearing phase can be explain only by variance of phase station of coexisting F-bearing fluid and connected variance of F activity.

**Phase distribution of ore elements**

At 800°C and P=1 kbar crystal phases are present in equilibrium with aluminosilicate melt. In experiments with REE silicates of rare earth elements have been observed: approximate formula as calculated to 3 atoms of (O) is  $[\text{Na}_{0.16}\text{Ca}_{0.05}(\text{REE})_{0.97}]_{1.18}\text{Si}_{0.71}\text{O}_3$ . Partition coefficients of elements  $K_i = (C_i^{\text{REE-sil}})/(C_i^{\text{AlSi-melt}})$  have been calculated, where  $C_i$  is content of element in mass/%; REE-sil – silicate of REE; AlSi-melt – aluminosilicate melt. It has been shown that Na and Si enrich melt while Ca, Y and REE concentrate in REE silicates. For the REE group  $K_i = (C_i^{\text{REE-sil}})/(C_i^{\text{AlSi-melt}})$  increases in order Y → Dy → Gd → La → Ce = 4.14 → 7.84 → 13.91 → 20.30 → 21.06.

Presence of phase-saturator in experimental products allows to estimate maximum contents of REE oxides in aluminosilicate glass (at 800°C and P=1 kbar):  $\text{Y}_2\text{O}_3$  – 1.61 mass.%;  $\text{La}_2\text{O}_3$  – 0.86 mass.%;  $\text{Ce}_2\text{O}_3$  – 0.94 mass.%;  $\text{Gd}_2\text{O}_3$  – 1.49 mass.%;  $\text{Dy}_2\text{O}_3$  – 1.40 mass.%. In experiments with additions of V, Nb, Ta oxides in the products pyrochlore-microlite and small (<1-2 mkm) drops of fluoride melt are obtained in equilibrium with aluminosilicate melt. Partition coefficients of number of elements between pyrochlore and aluminosilicate melt have been calculated. Na and K enrich aluminosilicate melt,  $K_i = (C_i^{\text{Pchl}})/(C_i^{\text{AlSi-melt}}) = 0.64$  and 0.18 respectively. F, Ca, V, Nb, Ta enrich pyrochlore (microlite) with respect to the melt. Values of  $K_i = (C_i^{\text{Pchl}})/(C_i^{\text{AlSi-melt}})$  increase in order V → F → Nb → Ta → Ca = 2.07 → 2.24 → 34.47 → 73.31 → 90.11. Concentrations of Nb and Ta oxides in aluminosilicate melt which is equilibrium with phase-saturator pyrochlore (microlite) are 1.11 and 0.55 mass.% respectively. In experiments with charge containing Ti, Zr, Hf in products phases  $\text{ZrSiO}_4$ ,  $\text{ZrO}_2$ ,  $\text{HfSiO}_4$  have been obtained. Maximum concentrations of Zr and Hf oxides in silicate glass (in presence of phasesaturators) have been estimated: 1.35 and 2.47 mass. %.

For experiments at 900°C (charge with REE) partition coefficients of REE between fluoride (F-f) and aluminosilicate (AlSi-melt) melts have been calculated:  $K_i = (C_i^{\text{F-f}})/(C_i^{\text{AlSi-melt}})$  (fig. 1). Following data have been obtained (experiments at 900°C and 1 kbar; data for P=2 kbar are given in brackets): for Y – 12.3(11.2); for La – 19.2(11.7); for Ce – 13.3(10.5); for Gd – 11.1(8.46); for Dy – 6.10(5.13). It is shown that for 2 kbar values of  $K_i$  are an average of 20 % less than for experiments at 1 kbar.

In experiments at 1200°C values of  $K_i = (C_i^{\text{F-f}})/(C_i^{\text{AlSi-melt}})$  (for REE group) practically don't depend on pressure (fig. 1), so later on the average values are given: for Y – 17.7; for La – 19.1; for Ce – 15.5; for Gd – 14.4; for Dy – 10.4. As compared these data to data obtained at 900°C we can see that values of partition coefficients for La and Ce practically don't change, but for the group of hard rare earth elements (including Y) values of  $K_i = (C_i^{\text{F-f}})/(C_i^{\text{AlSi-melt}})$  are an average of 37 relative % more. In experiments with additions of other groups of elements (V, Nb, Ta and Ti, Zr, Hf) at 1200°C and P=1 kbar (charge 1) melting phases are absent and at 2 kbar fluoride melting phase (mixture of villiaumite and cryolite melts) are observed only in experiments with V, Nb, Ta (charge 1). This fluoride phase doesn't content elements of this group. In experiments carried out at 1200°C and P=2 kbar (charge 2) with ore elements groups (V, Nb, Ta) and (Ti, Zr, Hf) fluoride phase is represented by villiaumite (NaF) melt and doesn't content these element groups.

### Conclusions

1. Phase composition of experimental products in the system granite melt – Na fluoride at 800÷1200°C and  $P = 1\div 2$  kbar is studied.

2. Partition coefficients of rare earth elements between granite melt and fluoride phase at 900÷1200°C and  $P = 1\div 2$  kbar have been obtained. It has been shown that REE enrich fluoride phase relative silicate melt.

3. Elements of groups (V, Nb, Ta) and (Ti, Zr, Hf) practically always prefer silicate melt relative fluoride melt.

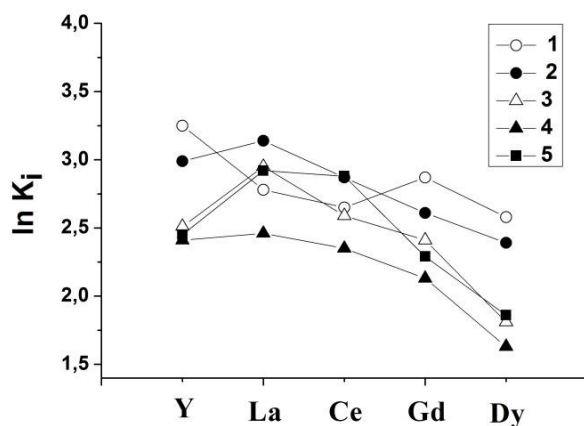


**Fig. 1. Distribution of REE between F-bearing phase (drops) and silicate glass.**

$K_i = (C_i^{\text{F-phase}}) / (C_i^{\text{glass}})$ , where  $C_i$  – element concentration.

1 – 1200°C, 1 kbar (charge 1); 2 – 1200°C, 2 kbar (загрузка 1); 3 – 900°C, 1 kbar; 4 – 900°C, 2 kbar; 5 – 1200°C, 2 kbar (charge 2).

This study was supported by RFBR, project № 15-05-03393.

*Authors are grateful to N.I. Kuznetsov and A. Terekhin for engineering and technical services and carrying out the experiments in high gas pressure vessel of IEM RAS.*